THE AMERICAN MINERALOGIST
JOURNAL OF THE MINERALOGICAL SOCIETY OF AMERICA

Vol. 26 APRIL, 1941 No. 4

# OPTICAL PROPERTIES AND CRYSTALLOGRAPHY OF ZONED PUMPELLYITE FROM THE WITWATERSRAND

J. E. DE VILLIERS, *Pretoria, Union of South Africa.*

ABSTRACT

Pumpellyite from the Witwatersrand was found to be intensely zoned and to show exceptionally wide variations in optical properties. Refractive indices ($\beta_D$) varied from 1.693 to 1.726, birefringences from .0016 to .0103 and optic axial angles ($2V_X$) from 38° [optic axial plane perpendicular to (010)] to 71° [optic axial plane parallel to (010)]. These angles again were dispersed through a wide range, showing $r>v$ in the former case and $r<v$ in the latter. The following axial elements were determined for the mineral: $\beta=70°$, $c/a=.842$.

## INTRODUCTION AND PHYSICAL PROPERTIES

Pumpellyite was first described by Palache and Vassar from the Lake Superior region in 1925. Since that time it has been found to be of fairly widespread occurrence, being reported from Haiti (Burbank, 1927), California (Irving, Vonsen and Gonyer, 1932), Eurasia (Waldmann,1934; Quitzow, 1935; Quitzow, 1936), Japan (Tsuboi, 1936), and New Zealand (Hutton, 1937). Up to the present a fair amount of work has been done on the chemistry[1] and such properties as the refractive indices and optic axial angles of pumpellyite, but to the writer's knowledge precise data on the crystallography and very interesting dispersion is still scanty. The present study was undertaken mainly with a view of determining the relations between the various optical and crystallographic properties of the Witwatersrand material.

During January, 1940, a small sample, stated to have come from the City Deep mine, Johannesburg, was submitted to the Geological Survey for identification. It consisted of aggregates of lustrous, greenish-black needles of pumpellyite in white vein quartz. Only about 1 gram of the mineral was available for study and all efforts to obtain a further supply have thus far proved unsuccessful. The specimens received were up to 1.5 cm. in diameter and were penetrated by coherent aggregates having a cross section of a few millimetres. The aggregates consisted of individual crystals, averaging about 1 mm. in diameter, in parallel or semi-parallel grouping. No terminating crystal faces were observed on the

[1] For a table of analyses see Irving, Vonsen and Gonyer (1932); also Tsuboi (1936).

needles but a series of prism faces, usually striated and somewhat rough, were present.

The pumpellyite was tentatively identified from its optical properties and a qualitative chemical analysis. In the optical measurements however certain serious divergencies from the known properties[2] of pumpellyite were found so that quantitative chemical data were required to place the identity of the mineral beyond doubt. Mr. C. F. J. van der Walt kindly undertook a partial analysis of about 350 milligrams of the cleaned mineral and obtained the following result: $SiO_2$ 36.9%, $Al_2O_3$ 27.7%, $Fe_2O_3$ (total) 9.0%, CaO 22.4%, MgO 1.0%. Total 97.0%. In addition 0.6% $B_2O_3$ was determined by the writer. The result shows a fairly good agreement with analyses of pumpellyite from other localities and although the percentage of alumina is somewhat high, this is probably due to the presence of an alteration product in the material analyzed.

The following physical properties were determined on the mineral: H. = ±6. G. = 3.226−3.318. Magnetism, weakly magnetic to the electromagnet. Crystals of pumpellyite removed from their quartz matrix were found to be unsuitable for accurate measurement on the goniometer and only one angle of about 63°, measured in the direction perpendicular to the elongation, appeared to be fairly constant.

About 15% of the mineral examined showed evidence of alteration, the final product being a semi-opaque, cryptocrystalline aggregate with a mean index of refraction of about 1.65. This material usually formed layers showing a rude parallelism with crystal outlines and cleavages and, in the small amount of material available, was impossible to separate satisfactorily by means of heavy liquids. Purification of the mineral for chemical analysis (apart from the removal of adhering quartz) was not attempted as it was further found that the heavier fractions were richer in fragments of comparatively high birefringence. Of the two values for the specific gravity given above, the lower figure represents the gravity of a small cleaned fragment and the higher that of the heaviest grains in a crushed sample. These figures were obtained by immersing the mineral in methylene iodide and diluting with acetone until neither floating nor sinking occurred. The specific gravity of the liquid was measured immediately and the result corrected for water at maximum density.

## Optical and Crystallographic Properties

Universal stage measurements on thin sections were in agreement with monoclinic symmetry, the direction of elongation of the prisms being the symmetry axis. Pleochroism was observed as follows: X = pale greenish-yellow, Y = blue-green, Z = brownish-yellow. Absorption Y > Z > X. The pleochroism was found to vary somewhat. For fragments showing the

[2] For a summary of the optical properties of pumpellyite see Hutton (1937).

highest interference colours, Y is a lighter green and the absorption of the Z and Y directions about equal. It is of interest to note here that Quitzow (1936) found the intensity of the colour of the mineral to vary with the strength of the dispersion.

Zoning parallel to the *b*-axis is marked and highly irregular although there is a tendency for the zones to show some parallelism with crystal outlines and for the mantles to have a higher birefringence than the cores. The zones may have sharply defined boundaries or grade into one another. At best, areas that are suitable for optical measurements may be .3 mm. in diameter, measured across the length of the crystals, but frequently fragments are so intricately zoned that they are completely unsuitable for such measurements. The ether axis corresponding to *b* is common for all zones in a single individual but any axis perpendicular to this may differ by as much as 32° from the corresponding axis in an adjacent zone.

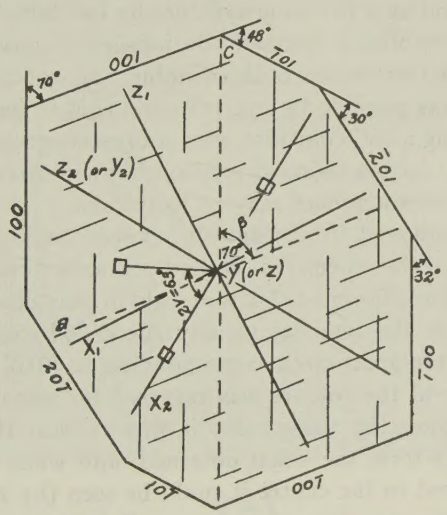


*Optic orientation of pumpellyite*

In thin sections cut parallel to (010) and accurately oriented by means of the universal stage, crystal outlines were more easily measurable than on the goniometer. Of the two imperfect cleavages observed, the better [considered as (001) after Palache and Vassar, 1925] was not found to correspond to a crystal face, while the other [considered as (100)] was paralleled by a well-developed face. The mean of a number of measurements for the angle between the cleavages gave a value of 70°. In addition hemiorthodomes ($\bar{1}01$) and ($\bar{2}01$), at angles of 48° and 78° respectively to (001), were noted. The positions of these faces and their relations to the optical directions are shown in Fig. 1.

On account of the imperfect development of the cleavages the accuracy of the crystallographic measurements is not considered to be greater than $\pm 2°$.

The axial elements of pumpellyite as far as these could be determined are thus as follows:

$$\beta = 70°$$

$$\frac{c}{a} = \frac{\sin (001 \wedge \bar{1}01)}{\sin (\bar{1}00 \wedge \bar{1}01)} = .842.$$

Twinning is fairly common in the material examined but difficult to distinguish from the ordinary zoning. The composition plane although somewhat irregular corresponds in general with (001) while a stereographic projection of the ether axes shows that the twinning axis may be either the pole of this face or the *a*-axis. It should be observed here that the possibility of finding a twinning axis for any two lamellae is not sufficient criterion to establish a twinned relationship as opposed to a zonal one. In the material examined both twinning and zoning occur in the [010] zone and it was possible to find twinning axes in both cases. Even where the "twinning axis" coincides with a crystallographic axis or the normal to a crystal face, a twinned relationship could not be said to be proved since the correspondence may be fortuitous.

The property employed to distinguish between zoning and twinning was the dispersion of the ether axes. When these axes were plotted on the stereographic net for different colours of light it was observed that the red and green of all the lamellae usually succeeded each other in the same direction on the great circle corresponding to [010]. In rare cases, however, the order of the colours was reversed for certain components as compared to others. In these cases it was evident that a different type of relationship from the usual obtained, and when the "twinning axis" was transferred to the centre it could be seen (by referring to the positions of the ether axes for red and green light) that only where the dispersion of one component was reversed relative to the other, the relationship was one of twinning.

It was further noted that in the cases where the dispersion indicated a twinned relationship the twinning axis was always the normal to (001) or the *a*-axis. In cases of zonal structure the "twinning axis" had no fixed direction.

Extinction angles and optic axial angles were measured in sections nearly perpendicular to X and the results are shown in graphical form in Fig. 2. In connection with these results it must be stated that especially in the measurement of extinction angles a high degree of accuracy was

unattainable. Cleavages even in what appeared to be the same zone sometimes diverged by as much as 8°. Optic axial angles larger than 40° were measured on the universal stage, while the smaller angles were measured by conoscopic observation according to Mallard's method. The

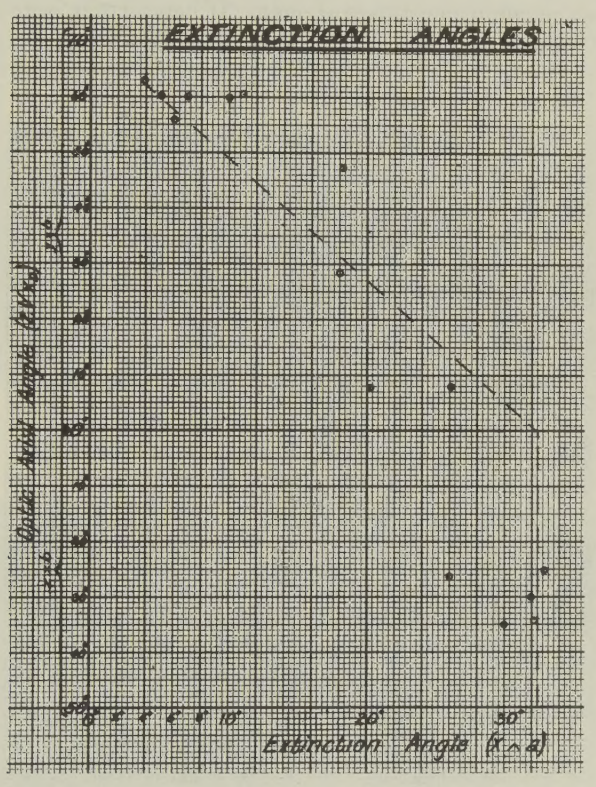


FIG. 2

accuracy is $\pm 2°$ for measurements on the universal stage and becomes progressively less as the optic axial angle and birefringence decrease. It is indeed extremely difficult even with a strong monochromatic light to distinguish the difference between 20° ($Y = b$) and 20° ($Z = b$). In rare cases it has been observed that the optic axial plane is apparently parallel to (010) for green light and perpendicular to it for red.

The extinction angle ($X \wedge a$) was found to vary from 4° to about 32° in the acute angle $\beta$. A relationship between the variables in Fig. 2 has been suggested by means of a line ruled on the graph. This may be stated as follows: "As the optic axial angle becomes smaller, one axis continuously

approaches the other which within small limits remains fixed. When zero is reached, the optic axial plane from being parallel to (010) becomes perpendicular to it and the position of the acute bisectrix remains more or less constant." Inspection of the optic axes in thin sections on the universal stage confirmed this statement. It has further been noted that the "fixed" optic axis is always the one that is least dispersed.

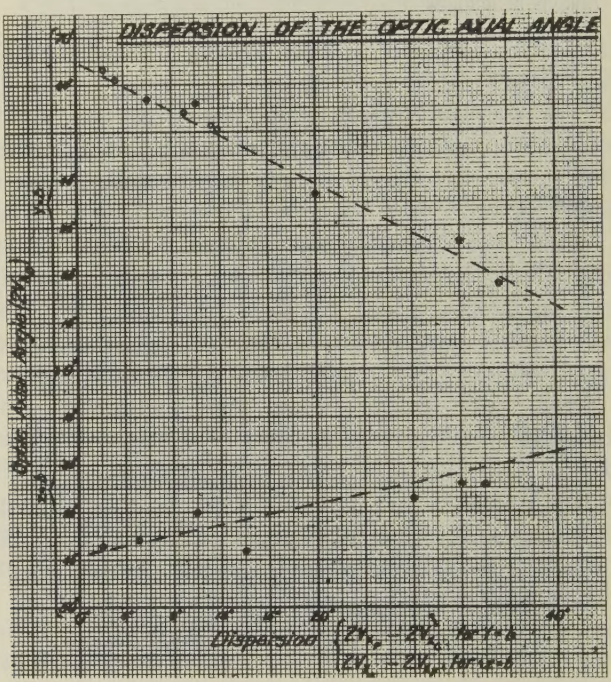


FIG. 3

## DISPERSION

Figure 3 shows graphically the measurements of the optic axial angle for different wavelengths. For determinations of $2V_D$ a sodium lamp was employed as light-source while for $2V_F$ and $2V_C$ Lifa filters Nos. 391 and 215, respectively, were used in conjunction with a microscope lamp.

The dispersion of the optic axes varies from 2°, when the optic axial angle is large and Z or $Y = b$, to about 35° when the angle approaches zero. The bisectrices were found to be dispersed about $\frac{1}{2}$° when the optic axial angle is large and $Y = b$ to about $4\frac{1}{2}$° when $Z = b$.

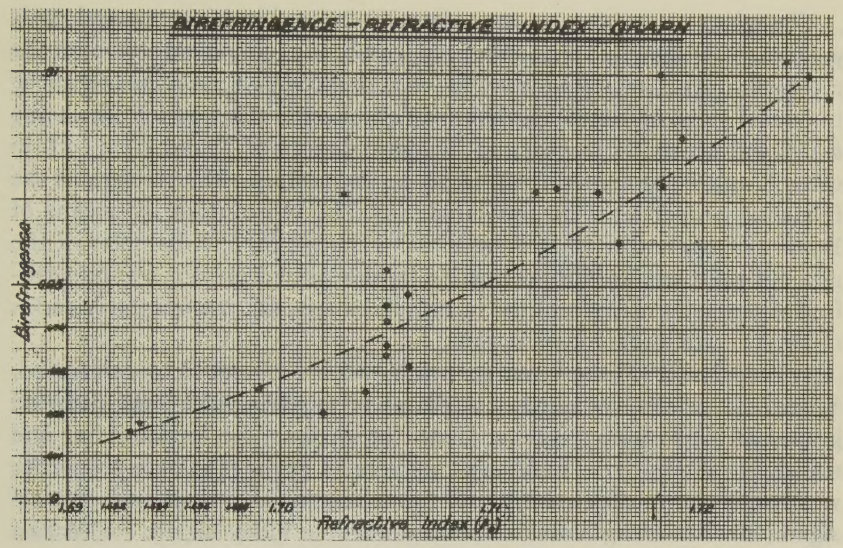
BIREFRINGENCE – REFRACTIVE INDEX GRAPH
Birefringence
Refractive Index (ε)

FIG. 4

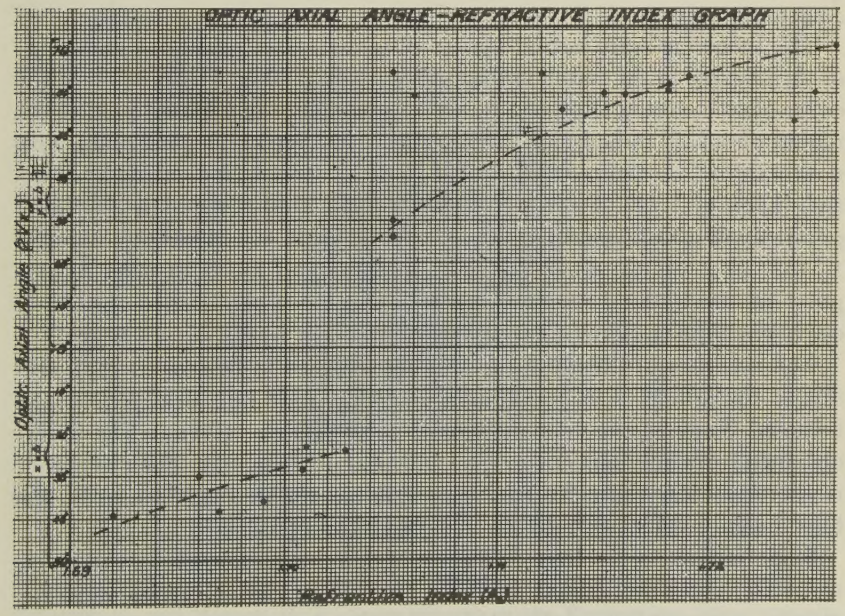
OPTIC AXIAL ANGLE – REFRACTIVE INDEX GRAPH
Refractive Index (ε)

FIG. 5

The relationship between the refractive index, birefringence and optic axial angle is shown in Figs. 4 and 5. To obtain these measurements the crushed mineral, mounted in hyrax, was investigated with the aid of the universal stage and monochromator. Grains were selected for which the *b*-axis was nearly horizontal and the optic directions X and Z (in certain cases X and Y) at angles of 40° to 50° to the vertical. On these grains the following properties were measured: (*a*) The retardation by means of Berek's compensator when Z or Y was vertical; (*b*) the diameter of the grain at right angles to this direction by means of a previously standardised micrometer ocular; (*c*) the optic axial angle; (*d*) the refractive index of the *b* crystallographic direction.

From (*a*) and (*b*) the birefringence $\beta-\alpha$ or $\gamma-\alpha$ could be calculated. Where $\beta-\alpha$ was obtained the complete birefringence was deduced graphically by taking into account the optic axial angle. After the measurements in hyrax had been completed a grain of known properties was removed from the mount and immersed in mono-iodonaphthalene. Again, the wavelength was read at which the index of the *b* direction equalled that of the immersion medium. With the aid of index dispersion curves of hyrax, mono-iodonaphthalene and pumpellyite it was then possible to deduce the refractive indices from the recorded readings in Ångstrom units.

The following were actual figures obtained. The refractive index ($\beta$) of the selected grain matched that of hyrax at 5850 Å. The portion of the cover-glass covering the grain was next removed, the exposed part of the mount dissolved in benzene and the grain recovered on a glass slide. This now matched with mono-iodonaphthalene at 4900 Å, indicating a refractive index of 1.727. From previously constructed dispersion graphs of pumpellyite it was found that at 5850 Å the grain would have an index of 1.7165. This was therefore the refractive index of hyrax at 5850 Å. One point on the hyrax dispersion curve having been established the whole curve could be constructed by referring to other hyrax curves near it.

The accuracy of these indices is not considered to be greater than .004 due to the difficulty in matching grains that were not ideally clear and unzoned. Further, the values of the optic axial angles given in Fig. 5 were obtained from only one optic axis and the acute bisectrix. Their accuracy is therefore less than the corresponding values in Figs. 2 and 3. For birefringence values a probable error of 15% is considered to apply.

Since indices lower than 1.702 could not be measured in the hyrax mount, ground sections of known orientation and thickness were immersed in mono-iodonaphthalene and the necessary optic angles, refractive indices and birefringences, to extend the graphs over the full range of refractive indices of the mineral, determined.

Dispersion graphs for the refractive index $\beta$ of pumpellyite were constructed by immersing selected grains successively in liquids of different index and determining their indices for different wavelengths. The information in the table below was obtained from these graphs.

| $\beta_D$ | $\beta_F - \beta_C$ |
|---|---|
| 1.6935 | .0140 (All $\pm$ .001) |
| 1.7055 | .0150 |
| 1.719 | .0155 |
| 1.720 | .0155 |
| 1.7265 | .0160 |

Inspection of Figs. 2–5 shows that in general no sharply defined relationship between the respective variables can be made out. Whilst the lack of symmetry is to a large extent certainly due to experimental error, the divergencies in some cases (notably Fig. 5) appear to be too large to be explained by such error. A possible explanation is that the unit cell of the pumpellyite investigated contains more than two variable constituents, but detailed chemical work on fractions of known optical properties is needed before a definite conclusion can be reached. In the present case unfortunately not enough of the material was available for this work to be carried out.

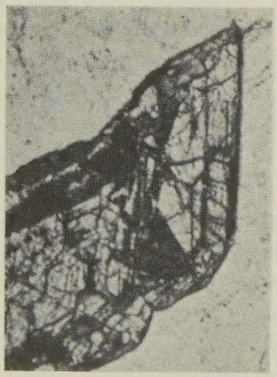

FIG. 6. **Section of pumpellyite** parallel to (010) in quartz matrix. Note crystal outlines and semi-opaque alteration product. ×56.

REFERENCES

PALACHE, C., and VASSAR, H. E., Some minerals of the Keweenawan copper deposits: pumpellyite, a new mineral; sericite; saponite: *Am. Mineral.*, **10,** 412–418 (1925).

BURBANK, W. S., Additional data on the properties of pumpellyite, and its occurrence in the Republic of Haiti, West Indies: *Am. Mineral.*, **12,** 421–424 (1927).

Irving, J., Vonsen, M., and Gonyer, F. A., Pumpellyite from California: *Am. Mineral.*, **17,** 338–342 (1932).

Waldmann, L., Pumpellyit aus Steiermark und Finnisch Lappland: *Min. Petr. Mitt.* (*Tschermak*), **45,** 92–93 (1934).

Quitzow, H. W., Diabas-Porphyrite und Glaukophangesteine in der Trias von Nordkalabrien: *Nachr. Gesell. Wiss. Göttingen, math.-phys. Kl., N.F.*, **1,** no. 9, 83–118 (1935).

Quitzow, H. W., Pumpellyit, ein häufiges Hydrothermal- und Sekundärmineral in basischen Gesteinen: *Zentr. Min., Abt. A*, 39–46 (**1936**).

Tsuboi, S., Petrological notes: *Japanese Jour. Geol. Geogr.*, **13,** 333–337 (1936).

Hutton, C. O., An occurrence of the mineral pumpellyite in the Lake Wakatipu region, western Otago, New Zealand: *Min. Mag.*, **24,** 529–533 (1937).

# MORPHOLOGY OF MECHANICAL TWINNING IN CRYSTALS

James Forbes Bell, *Massachusetts Institute of Technology, Cambridge, Mass.*

Abstract

The methods and results of morphological studies on mechanically twinned crystals are reviewed. The derivation of the formulae relating the indices of any face before and after mechanical twinning is presented. A new and direct graphic solution for the twinning elements in a crystal which has been subjected to a twinning deformation is developed.

## Introduction

As a result of the increasing interest in the interpretation of preferred orientations of the minerals in deformed rocks, the mechanism of the plastic deformation of minerals has become important to the structural geologist and the petrologist. There are two main types of plastic deformation in crystals. The first is known as translation-gliding. This is a mechanism whereby the crystal will deform by means of slip along certain planes and in certain directions. This mechanism does not produce a reorientation of the crystal structure. The second is known as twin-gliding which also takes place by means of slip along certain planes and in certain directions. This mechanism reorients the crystal structure to develop twinning. Both of these mechanisms are thought to play important roles in the development of preferred orientations in deformed rocks.

In 1930, M. J. Buerger (3)* undertook a study of translation-gliding. He compiled and evaluated all the work which had been done on this phenomenon in minerals. This served as a basis for new experiments designed to clarify and explain translation-gliding in the light of our present knowledge of crystal structure. The purpose of this paper is to make a similar study of *twin-gliding*. Most of the literature on the subject is in German and good bibliographies are not available. The writer feels that a paper dealing with the underlying principles and demonstrating the logical development of the theories of twin-gliding, which started over fifty years ago as a result of morphological studies and are still in use today, would serve as an adequate foundation for further work on the subject.

The application of the theory of simple shear to explain the phenomenon of twin-gliding, and the development of the transformation formulae (which are to be explained here on the basis of surface morphology), have been explained and derived on the basis of the Bravais crystal lattice. Since morphological studies are still the most important

* Numbers refer to corresponding references in the bibliography.

tool used in the determination of twin-gliding in mineral crystals, the writer feels that this approach to the subject is the most logical. It will also serve as a good foundation for discussions of the data which the writer is now compiling, as well as for future discussions of twin-gliding and its explanation on the basis of crystal lattices and crystal structures.

## History of the Study of Twin-Gliding

In 1826, Brewster (2) discovered that the lamellae which had often been observed in cleavage rhombohedrons of calcite were really due to twinning. Over thirty years later, in 1859, Pfaff (10) found that he could press a cleavage rhombohedron of calcite with a force perpendicular to two opposite edges and thereby change the orientation of the interference figure in parts of the crystal. However, it was not until 1867 that Reusch (11) recognized that the twinning described by Brewster and the changed interference due to pressure reported by Pfaff, were one and the same thing. This marks the beginning of the study of mechanical twinning (twin-gliding).

Following Reusch's recognition that twinning could be produced mechanically, mineralogists made extensive studies of the phenomenon during the late 1800's and the early 1900's. Since that time interest seems to have been lost in this phenomenon, or else it has been considered unimportant, because it is either omitted or given very incomplete treatment in most mineralogical textbooks and reference books. This is especially true of those books published in the English language.

During the last twenty years the metallurgists have found the behavior of metal crystals during deformation to be of increasing practical importance. As a result, extensive researches have been carried out on the twin-gliding and translation-gliding of metal crystals. Most of these studies have as their foundation the early work of the mineralogists. Consequently most of the modern theories of crystal deformation have been developed by the metallurgists (4, 13). These theories are limited by the material on which the metallurgists have worked, and also by lack of aid from the mineralogical data on twin-gliding, which for the most part had not even been compiled.

## Morphological Changes in a Crystal Due to Mechanical Twinning as Shown by Calcite

In spite of the fact that mechanical twinning has been produced in at least fifty different minerals, calcite is still used as the type example of mechanical twinning. This is due to several factors: the mineral is very common; in the second place, it can be twinned easily; in the third place, it is the only common mineral in which an easily obtainable form (the

cleavage rhombohedron) develops both morphological and structural symmetry as a result of mechanical twinning.

The familiar technique of producing twinning in a calcite rhombohedron by pressing a knife blade into the crystal was first described by Baumhauer (1) in 1879. Figure 1 copied from Johnson (5) illustrates this procedure. A wedge-shaped opening of constant angle develops under the knife blade. At the same time a triangular prismatic section of the crystal is displaced to the right. This displacement causes an apparent

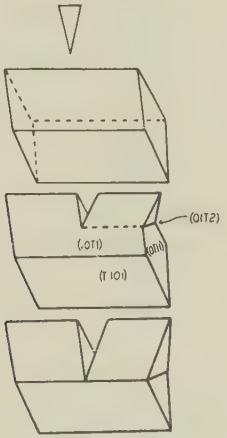


FIG. 1. Formation of a "knife blade" twin on a cleavage rhombohedron of calcite (modified after Johnson).

tipping of a section of the right hand face of the rhombohedron, forming a reentrant angle of constant value for that face. The tipped section of the right hand face remains an optically flat surface. The other two faces of the cleavage rhombohedron which bound the displaced triangular prism show no effects of the deformation. The contact between the displaced prism and the rest of the cleavage rhombohedron is a horizontal plane equivalent to the flat rhombohedron $(01\bar{1}2)$ in the original crystal. It is often possible to develop a good parting parallel to this plane and thereby determine its attitude on the goniometer.

If the faces on the deformed and undeformed parts of this cleavage rhombohedron are measured, and plotted on a stereographic projection, it is found that the displaced portion of the crystal and the undisturbed portion are symmetrical about this plane of separation $(01\bar{1}2)$. Crystallographically this relationship may be thought of as a 180° rotation of the displaced part about the normal to this plane or about an axis parallel to the horizontal edges of the cleavage rhombohedron (Fig. 2).

Optical studies show that this relationship is the same for the interference figures of the two parts of the crystal. It is, of course, obvious that the mechanically twinned portion of the crystal was not actually cut loose and turned 180° about either of these axes, just as natural twins are not actually rotated.

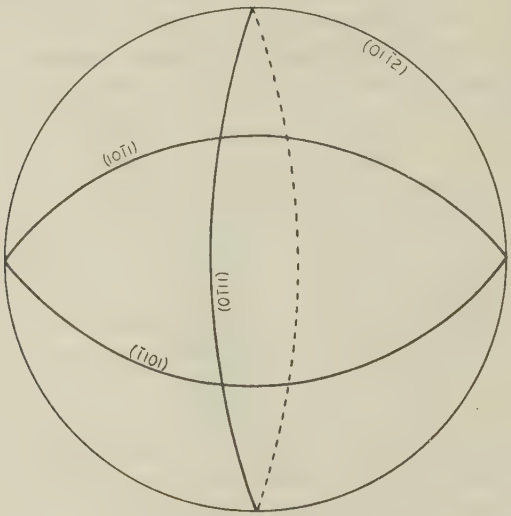


FIG. 2. Cyclographic projection of the "knife blade" twin illustrated in Fig. 1.

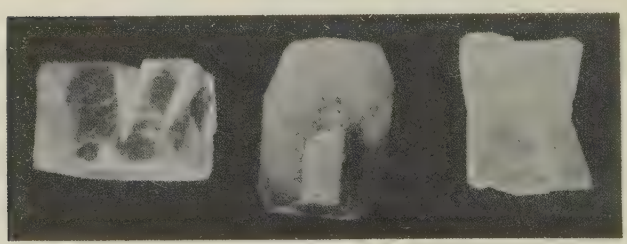

FIG. 3. (0112) twins in calcite; left: "knife blade" twin similar to those illustrated in Figs. 1 and 2. Center: twin-gliding lamellae on a crystal of calcite from Egremont, England. The crystal is bounded by cleavage rhombohedrons and prism faces. Compare with the projection Fig. 4. Right: growth twin from Guanajuato, Mexico.

If the calcite crystal is not bounded by the planes of the cleavage rhombohedron but for example by six prism faces terminated by the unit rhombohedron, as shown in Fig. 3, the twinning resulting from deformation is not so obvious. After deformation the crystal is cut by a series of lamellae. These lamellae are present in all of the faces except two

of the unit rhombohedron. Close examination shows that these lamellae bound tipped portions of the faces on which they appear. Although all of these tipped planes are optically flat, various physical tests have shown that in many cases they are not the same as their undeformed equivalents. The cyclographic projection* of this crystal showing all of the faces present after deformation (Fig. 4) does not show any symmetry in re-

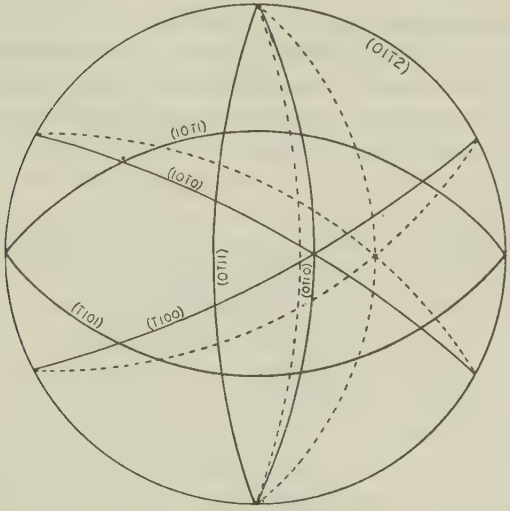


FIG. 4. Cyclographic projection of the faces present on the crystal shown in Fig. 3 (center). Note the lack of symmetry about (0112).

spect to the plane of the lamellae, although the projections of the rhombohedral planes are the same as they were in the case of the deformed cleavage rhombohedron (Fig. 2). The cleavage rhombohedron, therefore, must represent some unique form in calcite which shows mechanical twinning morphologically. Muegge (7, 8) recognized the presence of these unique forms in calcite as well as in other minerals. He realized that the displacement of any face on a crystal due to mechanical twinning must in some way be related to this so-called "grundform" and he thought that the mechanical twinning could probably be characterized by this "grundform." However, his attempt in 1885 (8) to set up analytical expressions for these relationships was unsuccessful.

## APPLICATION OF THE THEORY OF SIMPLE SHEAR TO MECHANICAL TWINNING

Simple shear is a homogeneous deformation which takes place by movements along a series of parallel planes (in a definite direction)

* A projection in which planes are represented by great circles on a stereographic net.

whereby each plane has exactly the same amount of displacement in respect to its neighbors as every other plane does in respect to its neighbors. A prosaic analogy would be the deformation of a deck of cards in which each card slides over its neighbor in a definite direction and by the same amount as every other card.

In a deformation of this kind there is no volume change, planes remain planes, straight lines remain straight lines and a sphere will become an ellipsoid. Let us imagine a plane perpendicular to the slip planes and parallel to the slip direction, through a sphere and the ellipsoid which is its deformed equivalent. Such a plane is called the plane of deformation and it is the plane of projection of the drawing in Fig. 5, which may be used to discuss this process of simple shear.

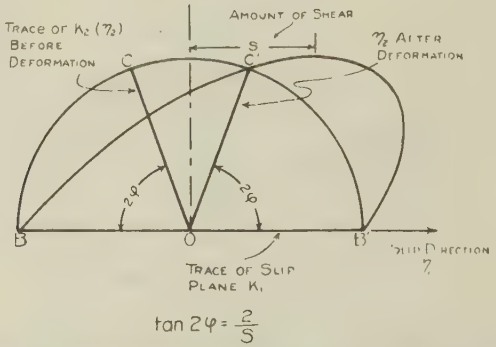


Fig. 5. Diagram illustrating simple shear. The plane of deformation is the projection plane.

The circle $BCC'B'$ with a radius equal to unity may for example be deformed into the ellipse $BC'B'$ by slip along a set of lines parallel to $BB'$. The ratio of the amount of displacement along any line to its perpendicular distance from $BB'$ is a constant for any particular deformation and is called the "amount of shear." This is designated by the letter $s$ and is equal to the displacement along a line at a unit distance above $BB'$. It is obvious that any simple shear could be uniquely defined by the slip plane, the slip direction and the amount of shear.

There are two planes in the ellipsoid, the circular cross-sections, which do not change in shape or size as a result of this deformation. These are represented by the lines $BB'$ and $OC$. $BB'$ does not change its position. $OC$ changes its position to that of $OC'$ and this change is a function of the amount of shear. The angle $2\phi$ between the slip plane $BB'$ and the other plane of no distortion $OC$ bears the following relation to the amount of shear: (13)

$$\tan 2\phi = \frac{2}{s}$$

The intersection of the two planes of no distortion is perpendicular to the slip direction. Therefore, it is also possible to uniquely define the simple shear by means of the two planes of no distortion and their included angle.

It is seen that the relationship of the two planes of no distortion before and after deformation can be geometrically described by a rotation of 180° of the original positions about an axis normal to the slip plane or about an axis parallel to the slip direction.

In 1889, Liebisch (6) realized that this theory of simple shear could be used as a geometrical means of describing the end result of mechanical twinning. In the knife blade twin of calcite, the deformation could be considered as the result of slip along a series of planes parallel to $(01\bar{1}2)$ with the slip direction parallel to the horizontal edge of the cleavage rhombohedron. In this case the right-hand face of the cleavage rhombohedron would be the other plane of no distortion and its symmetry in respect to the slip plane and the slip direction is explained. The homogeneity of this kind of deformation also explains the fact that all of the tipped planes remain optically flat. It also explains the fact that the tipped portions of planes which are not symmetrical to their original positions in respect to the slip plane no longer have the same properties as they had originally (etch figures). This theory of simple shear explains all of the facts which can be observed on mechanically twinned crystals. However, it should be emphasized that this may not represent the actual movements of atoms, molecules, ions or other units in the crystal structure.

## Transformation of Indices of a Face as a Result of Mechanical Twinning

After it was realized that the development of mechanical twins could be geometrically described as a simple shear, the next important problem was to find some way of using the tipped faces of a deformed crystal to define the twinning process. We have seen that a process of simple shear can be uniquely defined by the two planes of no distortion and their included angle. Therefore, if we know the indices of these two planes in a certain crystal we can describe the twin. It has also been shown that this twin will be geometrically equivalent to a 180° rotation about the normal to the slip plane or about the axis which is parallel to the direction of slip.

In 1889 Liebisch (6) and Muegge (10) developed the transformation formulae which relate the indices of an original crystal face to the indices

of its tipped portion in the twinned individual in terms of the indices of the planes of no distortion of the strain ellipsoid of simple shear. These transformation formulae can be developed in the following manner:

In crystallographic literature the slip plane is designated by $K_1$. The intersection of this plane with the plane of deformation is parallel to the slip direction and is designated by $N_1$. The other plane of no distortion is designated by $K_2$ and its intersection with the plane of deformation is designated by $N_2$.

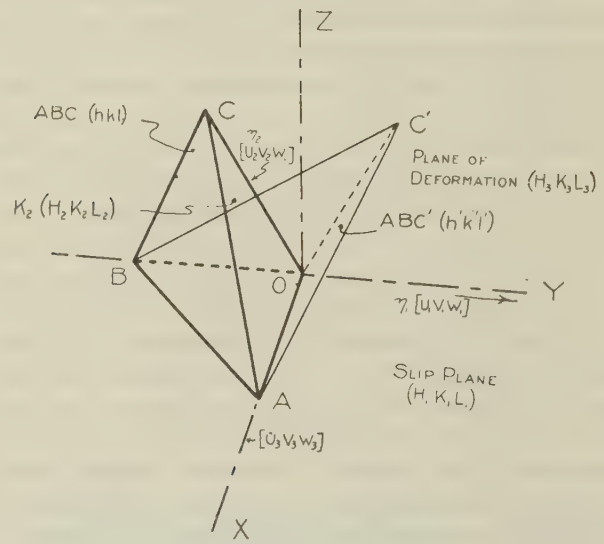


FIG. 6. Diagram illustrating the derivation of the transformation formulae.

Let us refer a crystal which shows twin-gliding to a set of rectangular coordinates, $X$, $Y$, $Z$, Fig. 6, in such a manner that the $XY$ plane coincides with $K_1$, and the $YZ$ plane coincides with the plane of deformation. $OY$ is then parallel to $N_1$ and $OX$ is perpendicular to $N_1$ in the slip plane $K_1$. Let $OC$ and $OC'$, which lie in the plane of deformation, be parallel to $N_2$ before and after deformation respectively. $OCX$ and $OC'X$ then represent $K_2$ before and after deformation. Let the plane $ABC$ represent any plane in the crystal before deformation. After deformation it will occupy a position and attitude indicated by $ABC'$.

Let the indices in respect to the undeformed crystal axes of the elements which we have just described be:

| | |
|---|---|
| $ABC$, any plane before deformation | $(hkl)$ |
| $ABC'$, any plane after deformation | $(h'k'l')$ |
| $K_1$, the slip plane | $(H_1K_1L_1)$ |

| | | |
|---|---|---|
| $K_2$, | the other plane of no distortion | $(H_2K_2L_2)$ |
| $N_1$, | the slip direction | $[u_1v_1w_1]$ |
| $N_2$, | | $[u_2v_2w_2]$ |
| $OX$, | intersection of $K_1$ and $K_2$ | $[u_3v_3w_3]$ |
| $YZ$, | plane of deformation | $(H_3K_3L_3)$ |

It is now possible to refer the plane $ABC$ with indices $(h, k, l)$ to a new set of axes. Let these new axes be $OX$, $OY$, and $OC$ as the $a$, $b$, and $c$-axes respectively.

By cross multiplication we find that the indices of the new axial planes are:

$$\begin{aligned}
&(H_3K_3L_3) \text{ of } YZ=((v_1w_2-v_2w_1)(u_2w_1-u_1w_2)(u_1v_2-u_2v_1))\\
&(H_2K_2L_2) \text{ of } K_2=((v_2w_3-v_3w_2)(u_3w_2-u_2w_3)(v_1w_3-u_3w_1))\\
&(H_1K_1L_1) \text{ of } K_1=((v_3w_1-v_1w_3)(u_1w_3-u_3w_1)(u_3v_1-u_1v_3))
\end{aligned} \tag{1}$$

The transformation formulae for this change are:

$$\rho\cdot h_0=\frac{hu_3+kv_3+lw_3}{\theta_3}, \qquad \theta_3=(u_3+v_3+w_3)$$

$$\rho\cdot k_0=\frac{hu_1+kv_1+lw_1}{\theta_1}, \qquad \theta_1=(u_1+v_1+w_1) \tag{2}$$

$$\rho\cdot l_0=\frac{hu_2+kv_2+lw_2}{\theta_2}, \qquad \theta_2=(u_2+v_2+w_2)$$

where $h_0$, $k_0$, $l_0$ are the indices of the plane $(hkl)$ referred to new axes $[u_3v_3w_3]$, $[u_1v_1w_1]$ and $[u_2v_2w_2]$ and $\rho$ is a proportionality factor.

By solving the three equations (2) for $h$, $k$ and $l$ we get:

$$\begin{aligned}
\rho\cdot h&=\theta_3h_0(v_1w_2-v_2w_1)+\theta_1k_0(v_2w_3-v_3w_2)+\theta_2l_0(v_3w_1-v_1w_3)\\
\rho\cdot k&=\theta_3h_0(u_2w_1-u_1w_2)+\theta_1k_0(u_3w_2-u_2w_3)+\theta_2l_0(u_1w_3-u_3w_1)\\
\rho\cdot l&=\theta_3h_0(u_1v_2-u_2v_1)+\theta_1k_0(u_2v_3-u_3v_2)+\theta_2l_0(u_3v_1-u_1v_3)
\end{aligned} \tag{3}$$

These formulae give the original indices of the faces in terms of the indices referred to the axes $OX$, $OY$, and $OC$.

By substituting values from (1) equations (3) may be expressed:

$$\begin{aligned}
\rho\cdot h&=\theta_3h_0H_3+\theta_1k_0H_2+\theta_2l_0H_1\\
\rho\cdot k&=\theta_3h_0K_3+\theta_1k_0K_2+\theta_2l_0K_1\\
\rho\cdot l&=\theta_3h_0L_3+\theta_1k_0L_2+\theta_2l_0L_1
\end{aligned} \tag{3a}$$

The discussion of the strain ellipsoid has shown that the deformed equivalents of the axes $OX$, $OY$ and $OC$ will be $-OX$, $-OY$ and $OC'$ or $-OX$, $OY$ and $-OC'$ depending upon whether we choose an axis of rotation normal to $K_1$ or parallel to $n_1$ in describing the deformation. In either case, the relationship of the crystallographic axis in the new position to the new positions of the axes $OX$, $OY$ and $OC$ will be the same as the relationship between these two sets of axes in the original positions.

Therefore, the formulae

$$\begin{aligned}\rho\cdot h' &= \theta_3 h_0' H_3 + \theta_1 k_0' H_2 + \theta_2 l_0' H_1\\ \rho\cdot k' &= \theta_3 h_0' K_3 + \theta_1 k_0' K_2 + \theta_2 l_0' K_1\\ \rho\cdot l' &= \theta_3 h_0' L_3 + \theta_1 k_0' L_2 + \theta_2 l_0' L_1\end{aligned} \tag{4}$$

express the relationship between the indices $h'k'l'$ of the plane $ABC'$ referred to the new crystallographic axes and its indices referred to the deformed equivalents of $OX$, $OY$ and $OC$.

Let us first consider the deformation as equivalent to a rotation of the axes 180° about the normal to $K_1$. In this case, $OX$ is equivalent to $-OX$, $OY$ is equivalent to $-OY$ and $OE$ is equivalent to $OE'$ in the new positions. Therefore the indices of the plane $ABC'$ are:

$$h_0 = -h_0',\ k_0 = -k_0' \quad \text{and} \quad l_0 = l_0'. \tag{5}$$

Substituting the values of (5) in equation (4) we find:

$$\begin{aligned}\rho\cdot h' &= -\theta_3 h_0 H_3 - \theta_1 k_0 H_2 + \theta_2 l_0 H_1\\ \rho\cdot k' &= -\theta_3 h_0 K_3 - \theta_1 k_0 K_2 + \theta_2 l_0 K_1\\ \rho\cdot l' &= -\theta_3 h_0 L_3 - \theta_1 k_0 L_2 + \theta_2 l_0 L_1\end{aligned} \tag{6}$$

If we now substitute the values of $h$, $k$ and $l$ from (2) in (6), we find that:

$$\begin{aligned}\rho\cdot h' &= 2H_1(u_2h+v_2k+w_2l) - h(u_2H_1+v_2K_1+w_2L_1)\\ \rho\cdot k' &= 2K_1(u_2h+v_2k+w_2l) - k(u_2H_1+v_2K_1+w_2L_1)\\ \rho\cdot l' &= 2L_1(u_2h+v_2k+w_2l) - l(u_2H_1+v_2K_1+w_2L_1)\end{aligned} \tag{6a}$$

We have now expressed the transformation of indices of any plane due to twin-gliding in terms of the original indices of the face, the indices of $N_2$ and the indices of $K_1$.

If on the other hand we consider the deformation as equivalent to a 180° rotation of the axes about $N_1$ then the indices of the plane $ABC'$ are:

$$h_0 = -h_0',\ k_0 = k_0' \quad \text{and} \quad l_0 = -l_0'. \tag{7}$$

Substituting these values in equation (4) we find:

$$\begin{aligned}\rho\cdot h' &= -\theta_3 h_0 H_3 + \theta_1 k_0 H_2 - \theta_2 l_0 H_1\\ \rho\cdot k' &= -\theta_3 h_0 K_3 + \theta_1 k_0 K_2 - \theta_2 l_0 K_1\\ \rho\cdot l' &= -\theta_3 h_0 L_3 + \theta_1 k_0 L_2 - \theta_2 l_0 L_1\end{aligned} \tag{8}$$

If we now substitute the values of $h_0$, $k_0$ and $l_0$ from (2) in (8), we find that:

$$\begin{aligned}\rho\cdot h' &= 2H_2(u_1h+v_1k+u_1l) - h(u_1H_2+v_1K_2+w_1l_2)\\ \rho\cdot k' &= 2K_2(u_1h+v_1k+u_1l) - k(u_1H_2+v_1K_2+w_1l_2)\\ \rho\cdot l' &= 2L_2(u_1h+v_1k+u_1l) - l(u_1H_2+v_1K_2+w_1l_2)\end{aligned} \tag{8a}$$

Here we have expressed the transformation due to twin-gliding of the indices of any plane in terms of the original indices of the plane, the indices of $N_1$ and the indices of $K_2$.*

* The use of these transformation equations can be illustrated by using calcite as an example. Let $K_1$ be $(01\bar{1}2)$. The corresponding $K_2$ is $(0\bar{1}11)$ and $S$ is $(2\bar{1}\bar{1}0)$. The intersection of $S$ with $K_1$ is $N_1$ $[12\bar{3}1]$ and with $K_2$ is $N_2$ $[12\bar{3}2]$. For use in the transformation equations only 3 indices are used. For these elements they are: $K_1=(01.2)$, $K_2=(0\bar{1}.1)$, $S=(2\bar{1}.0)$, $N_1=[12.\bar{1}]$, $+N_2=[12.2]$.

If we now investigate the transformation of the plane $(02\bar{2}1)$ due to twin-gliding with the above-mentioned elements we find:

By means of these transformation formulae we can express the morphological changes which take place in a crystal as a result of mechanical twinning. It has been shown that these twins can be described by a rotation about one of two axes. Observers have found that in some cases the slip plane has simple indices, and then it can be considered as the twin plane or its normal as the twin axis. This is known as *TWINNING OF TYPE I.* In other cases the slip plane is irrational, but the slip direction, $N_1$, is rational and can be considered as the twin axis. This is known as *TWINNING OF TYPE II.* It should be emphasized that from a morphological standpoint these two types of twinning are identical except for the so-called rationality or irrationality of certain elements used in our geometrical description of mechanical twinning. In some cases all of the elements used to describe a mechanical twin are rational. If this is the case, it often happens that $K_2$ may also function as a slip plane, whereby two varieties of twins will be formed. One variety can be described as twinning by rotation about the normal to $K_1$ or about $N_1$. The other can be described by rotation about the normal to $K_2$ or about $N_2$. This is called *RECIPROCAL TWINNING.*

There are hundreds of measurements on record which show the validity of the transformation formulae which have been developed. If the indices of two faces which do not lie in the same zone are known before and after the deformation, it is possible to solve these formulae for $K_1$ and $N_2$ or for $K_2$ and $N_1$. However, if we do not know what the twin plane in a crystal is, it is impossible to index any faces with respect to the twinned axes. Most investigators have been able by close observation and shrewd guessing to arrive at probable values for $K_1$, $K_2$, $N_1$, and $N_2$. After doing this they substituted these values in the transformation formulae and found what the indices of the displaced faces should be. It was then a simple matter to measure the angles between the displaced faces

---

By substituting the values for $K_1(H_1=0,\ K_1=1,\ L_1=2)$, $N_2(u_2=1,\ v_2=2,\ w_2=2)$ and $h=0,\ k=2,\ l=1$ in equation (6*a*) we find that:

$$\rho\cdot h'=0(0+4+2)-0(0+2+4)=\ 0$$
$$\rho\cdot k'=2(0+4+2)-2(0+2+4)=\ 0$$
$$\rho\cdot l'=4(0+4+2)-1(0+2+4)=18$$

Dividing through by the proportionality factor, $\rho=18$, $h'k'l'$ become (001).

By substituting the values for $K_2(H_2=0,\ K_2=-1,\ L_2=1)$, $N_1(u_1=0,\ v_1=2,\ w_1=-1)$ and $h=0,\ k=2,\ l=1$ in equation (8*a*) we find that:

$$\rho\cdot h'=0(0+4-1)-0(0-2-1)=0$$
$$\rho\cdot k'=-2(0+4-1)-2(0-2-1)=0$$
$$\rho\cdot l'=2(0+4-1)-1(0-2-3)=9$$

Dividing through by the proportionality factor, $\rho=9$, $h'k'l'$ become (001).

This shows that with these deformation elements $(02\bar{2}1)$ becomes (0001) in the twinned crystal. This fact was established experimentally by Muegge in 1883 (7).

and their equivalent faces in the undeformed crystal. These values could be compared with those values which were calculated for the angles between the known indices of the original crystal face and the assumed indices in the twinned individual. The agreement between the calculated and the measured values served to substantiate or disprove their guess as to the values of $K_1$, $K_2$, $N_1$, and $N_2$. The transformation formulae, therefore provide an excellent means of checking, but only an indirect solution for the twinning elements.

## Graphic Solution of the Twinning Elements in Deformed Crystals with the Aid of the Stereographic Projection

It has been shown that a simple shear and thereby a mechanical twin can be completely described by three elements, namely:

(1) The slip plane ($K_1$)
(2) The slip direction in the slip plane ($N_1$)
(3) The amount of slip or shear ($s$).

If these three elements are known and their relation to the crystallographic axes of a crystal are known, then the twinning elements which developed during the deformation of a crystal are completely defined.

These three elements can be determined graphically. In order to do this one must know the positions with respect to the *original* crystal axes of two planes of a crystal before and after the twinning deformation. These two planes must not lie in the same zone and neither of them can be in the zone of the slip direction. The planes may be crystal faces or they may be artificially prepared planes. The only further restriction is that they give reflections which can be measured accurately on the reflection goniometer, or that they are suitable for measurement by other means.

From the data described above and illustrated in Fig. 7, the steps in the graphic solution are as follows:

(1) Plot the two planes before deformation (planes $A$ and $B$) and the corresponding planes after deformation (planes $A'$ and $B'$) as great circles on the stereographic net along with the crystallographic axes of the original crystal.
(2) The intersection of planes $A$ and $A'$ (point 1) and the intersections of planes $B$ and $B'$ (point 2) must both lie in the slip plane. Therefore the slip plane can be constructed as a great circle passing through these two points. The fact that the intersections of these planes lie in the slip plane is clear when we remember that in mechanical twinning the slip plane separates the deformed and undeformed parts of the crystal (see Fig. 1).
(3) The line of intersection of planes $A$ and $B$ (point 3) and the line of intersection of planes $A'$ and $B'$ (point 4) must lie in a plane which contains the slip direction. Therefore a great circle drawn through these two points will intersect the slip plane in a point which represents the slip direction (point 5).
(4) A great circle is then constructed parallel to the slip direction and perpendicular to the slip plane. This great circle represents the plane of deformation. The plane of deformation will intersect planes $A$, $A'$ and $B'$ in four points (points 6, 7, 8, and 9).

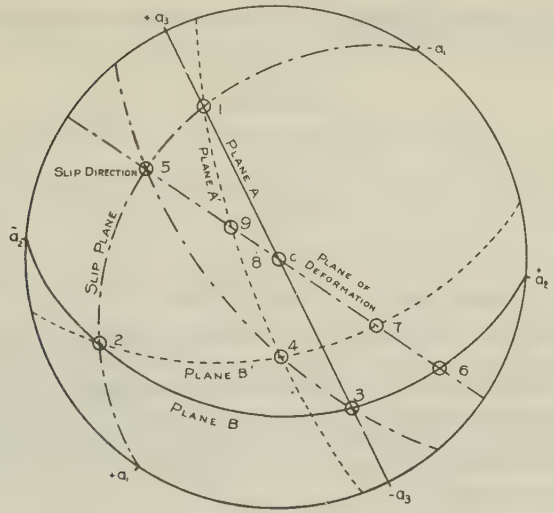


FIG. 7. Cyclographic projection of a mechanical twin in calcite illustrating the graphic solution for twin-gliding elements.

(5) The amount of shear can be calculated from the angles between the slip direction and the intersection of the planes of deformation with one of the planes before deformation ($\theta_1$) and the angle between the slip direction and the intersection of the plane of deformation with the same plane after deformation ($\theta_2$). The formula used in this calculation is:

$$s = \operatorname{ctg} \theta_1 - \operatorname{ctg} \theta_2.$$

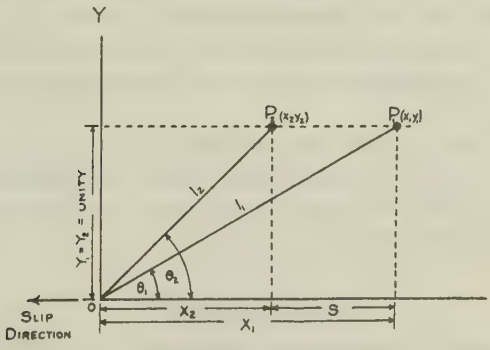


FIG. 8. Diagram illustrating how the amount of shear ($s$) may be derived from the graphic solution.

The derivation of this formula can be explained with the aid of Fig. 8. The plane of deformation is again the plane of the projection. The slip direction is parallel to $OX$. By simple shear, the point $P_1$ is transferred to the position of point $P_2$. If we consider

that their $y$ coordinate is equal to unity then the difference between their $x$ coordinates is equal to $s$. It follows that:

$$s = x_1 - x_2$$
$$x_1 = l_1 \cos \theta_1$$
$$l_1 = \frac{1}{\sin \theta_1}$$

so $$x_1 = \operatorname{ctg} \theta_1$$

similarly

$$x_2 = \operatorname{ctg} \theta_2$$

$$\therefore \quad s = \operatorname{ctg} \theta_1 - \operatorname{ctg} \theta_2.$$

From the value of $s$ we can calculate the angle between $K_1$ and $K_2$ and then we can plot $K_2$ and $N_2$ on the projection. We have now determined all of the elements necessary to describe a mechanical twin. The accuracy of our determination is limited only by the accuracy of the measurements and the accuracy of plotting. This graphic solution of the twinning elements is advantageous because it is direct and rapid and it helps to visualize the deformation. For final determinations the graphic solution can be checked by using the transformation formulae.

## Conclusions

From a review of morphological studies it has been shown that mechanical twinning in crystals may be described as a process of simple shear. However, it is to be emphasized that at present this process of simple shear cannot be applied to an analysis of the actual paths of movement of atoms, ions or molecules in the crystal during the deformation by twinning.

Formulae relating the indices of a crystal face before and after mechanical twinning to the elements of the deformation are reviewed. It has been pointed out that these transformation formulae cannot be used as a direct solution for the elements of the twinning deformation.

A new and direct graphic solution of the deformation elements has been presented.

Although much of the material presented in this paper is not original, it is the first time that it has been compiled in English in the present form. The writer feels that such a presentation is a necessary foundation for further studies of mechanical twinning.

## Acknowledgments

The writer wishes to express his gratitude to Dr. M. J. Buerger, Dr. J. T. Norton, Dr. H. W. Fairbairn and Mr William Parrish of the Massachusetts Institute of Technology for many helpful suggestions as well as for critical reading of this manuscript. The writer is also indebted to Dr. Harry Berman of Harvard University for his willing coöperation and interest as well as for the loan of several specimens of calcite.

This work was carried out under a Fellowship from the National Research Council to whom the writer wishes to express his appreciation.

## References

1. Baumhauer, H., Ueber Kuenstliche Kalkspath-Zwillinge nach $-\frac{1}{2}$ R.: *Zeits. Krist.*, **3**, 588 (1879).
2. Brewster, D., On a new cleavage in calcareous spar with a notice of a method of detecting secondary cleavage in minerals: *Ed. Jour. Sci.*, **9**, #18 (Apr.–Oct.), 311–314 (1826).
3. Buerger, M. J., Translation gliding in crystals: *Am. Mineral.*, **15**, 1 (1930).
4. Elam, C. F., Distortion of metal crystals: *Oxford at the Clarendon Press* **(1935)**.
5. Johnson, A., Schiebungen und Translationen in Kristallen: *Jahrb. der. Radio-aktivitaet u. Elektronik* **11**, 226 (1914).
6. Liebish, Th., Ueber eine besondere Art von homogenen Deformationen: *Neues Jb. Min., BB.* **6**, 105 (1889).
7. Muegge, O., Beitraege zur Kenntniss der Strukturflaechen des Kalkspathes und ueber die Beziehung derselben untereinander und zur Zwillingsbildung am Kalkspath und einigen anderen Mineralien: *Neues Jb. Min.*, **I**, 32 (1883).
8. Muegge, O., Zur Kenntniss der durch sekundaere Zwillingsbildung bewirkten Flaechenverschiebung: *Neues Jb. Min.*, **2**, 44 (1885).
9. Muegge, O., Zur Kenntniss der Flaechenveraenderungen durch sekundaere Zwillingsbildung II: *Neues Jb. Min.*, **1**, 136 (1886).
10. Muegge, O., Ueber durch Druck entstehendene Zwillinge von Titanit nach den Kanten (110) und (1$\bar{1}$0): *Neues Jb. Min.*, **2**, 98 (1889).
11. Pfaff, F., Versuche ueber den Einfluss des Drucks auf die optischen Eigenschaften doppeltbrechenden Krystalle: *Pogg. Ann.*, Ser. IV, Bd. **18**, 598 (1859).
12. Reusch, E., Ueber eine besondere Gattung von Durchgaengen im Steinsalz und Kalkspath: *Pogg. Ann.*, Ser. V, Bd. **17**, 441 (1867).
13. Schmid, E., and Boas, W., Kristallplastizitaet, mit besonderer Berueksichtigung der Metalle: J. Springer, *Berlin* **(1935)**.

# PARAGENESIS OF THE PEGMATITE MINERALS OF STRIEGAU, SILESIA

WILSON D. MICHELL, *Harvard University, Cambridge, Mass.*

ABSTRACT

Pegmatite bodies within a granite mass at Striegau, Silesia, contain a great number of open druses, in which were deposited most of the minerals forming the basis of this study.

Five stages of mineralization are established for the Striegau pegmatites. The first, or magmatic, stage included the formation of the main quartz-feldspar pegmatite bodies, and the graphic intergrowth of quartz and orthoclase surrounding the druses. The cavities were probably formed during the second, or albitization, stage, during which albite and cleavelandite were deposited in the druses and replaced some of the orthoclase of the druse walls.

Chlorite (strigovite, prochlorite, and penninite), tourmaline, fluorite, epidote, clinozoisite, and axinite belong to the succeeding period of druse filling. Pneumatolytic and hydrothermal action are indicated.

Zeolites, chiefly stilbite, are characteristic of the fourth stage of mineralization, which was evidently a period of cooling thermal solutions. Calcite crystals in the cavities represent the final period of mineral formation.

A table of mineral paragenesis is presented.

## GENERAL GEOLOGICAL RELATIONSHIPS

The Striegau intrusive granite mass is located about 60 kilometers southwest of Breslau in Prussian Silesia, at the eastern end of the Riesengebirge. The minerals forming the subject of this study were obtained from pegmatitic druse-bearing lenses in the Striegau granite mass.

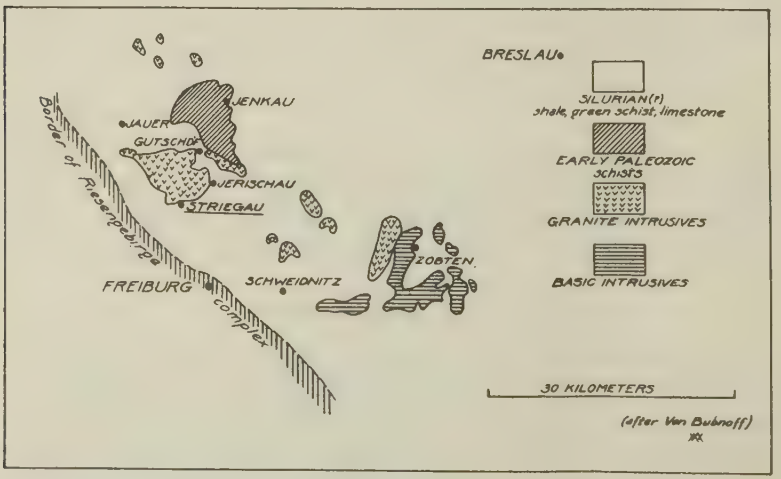


FIG. 1. Sketch map of the Striegau region, Silesia.

The intrusive is in the shape of a wedge pointing northwest, and has its greatest dimension, about 15 kilometers, in that direction (Fig. 1). The granite is in contact with gabbro and gneiss to the south; in the northeast it lies beneath the northwest-striking Jenkau schists of early Paleozoic age. The other surrounding rocks are shales, green schists, and limestones of Silurian(?) age. Where the granite touches schists and slates a distinct contact zone, high in tourmaline, has been developed. According to Cloos (quoted by Von Bubnoff, 1930), the Striegau granite was intruded along the gneiss-schist contact (Fig. 2).

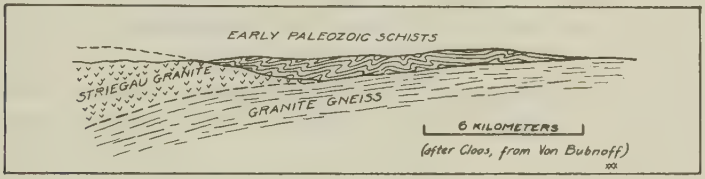


Fig. 2. Diagram to illustrate the possible mode of intrusion of the Striegau granite.

A lineation, trending northeast-southwest, has been observed in the granite. This lineation is nearly perpendicular to the elongation of the intrusive mass, but it is parallel to the regional structure.

The age of the Striegau granite has not been definitely determined, although it is perhaps late Carboniferous (Von Bubnoff, 1930, p. 538).

The granite of the Striegau intrusive is light colored and medium-grained to fine-grained. The chief constituents are white feldspar (principally potash feldspar, with subordinate plagioclase), gray quartz, and biotite. Muscovite is almost completely absent (Schwantke, 1896, pp. 2–3). Von Bubnoff (1930, p. 538) cites three sub-types of the granite: (1) coarse-grained biotite granite; (2) fine-grained acid granite; (3) some binary granite (this in contradiction to the statement of Schwantke).

The granite has a marked tendency to break readily along three mutually perpendicular planes, one nearly horizontal, the others approximately vertical and trending north-south or northwest-southeast (*Kopfabgänge*), and east-west (Schwantke, 1896, p. 3; Von Bubnoff, 1930, p. 538; Gürich, 1920, p. 310). This characteristic makes for easy quarrying and working of the rock, and the result is that a great number of quarries have been opened in the granite, permitting a rather thorough examination of its character.

The pegmatites contained in the granite are most abundant between Striegau and nearby Gräben. At Striegau the pegmatites are of two

principal types: (1) vein-like bodies about 6 inches wide with parallel walls, discontinuous along strike and dip, and in many instances associated with aplites; (2) nearly horizontal, sheet-like, irregular bodies (Gürich, 1920, p. 309). The pegmatites consist of feldspar and quartz predominantly; in some there are fairly large mica sheets. Feldspar is by far the most abundant mineral. These pegmatites contain the open druses in which were deposited most of the minerals discussed here. Some pegmatite lenses, however, contain no druses.

The druses attain a diameter of as much as 1 meter (Gürich, 1920, p. 310), and they may contain large, detached, smoky quartz crystals associated with loose fragments of feldspar and epidote. The walls are made up of spiky quartz crystals with interstitial potash feldspar, all overgrown by albite.

In addition to the pegmatites, the Striegau granite contains numerous other inclusions (Gürich, 1920, p. 310; Schwantke, 1896, pp. 3–4). Aplites are associated with the pegmatites. Quartz veins are found near or along the contact of the granite with the schist. Fracture fillings (generally in the nearly vertical *Kopfabgänge*) consist of quartz, fluorite, pyrite, chabazite, and calcite. Basic inclusions, of minor importance, are believed to represent altered schist fragments. There are also small lenses of muscovite, molybdenite, and hematite.

## Striegau Pegmatite Minerals

A brief discussion of the individual pegmatite minerals follows. The minerals are arranged as nearly as possible in their order of deposition. General paragenesis and the various stages of deposition are considered later.

### *Biotite*

Laths of biotite are intergrown with the graphic quartz and feldspar which constitute the base upon which the druse minerals are deposited. It appears, therefore, that the graphic quartz-feldspar and the biotite are part of the earliest, or magmatic, stage of pegmatite formation and make up the bulk of the pegmatite bodies.

Biotite deposition seems to have been essentially contemporaneous with the formation of the graphic quartz and feldspar. The biotite is in shreds and long laths and is generally oriented with the flamboyant structure of the enclosing graphic intergrowth. Some biotite, however, follows cracks which cut across the graphic structure. Biotite of this early stage of deposition is of the green variety, and is relatively fresh, showing alteration to chlorite only rarely.

Biotite which appears to be of a later stage of deposition is found associated with albite and quartz. This biotite is strongly pleochroic, green to brown, and is considerably altered to chlorite and epidote.

The biotite of both stages of deposition, and especially of the later stage, is found only in small amounts in the specimens.

*Orthoclase*

Orthoclase, in graphic intergrowth with quartz, is the principal constituent of the pegmatite material which surrounds the druses.

The orthoclase is almost universally micro-perthitic. The perthitic intergrowth, however, is rarely distinct, and serves only to make the orthoclase in thin section appear cloudy or dirty. In a few cases distinct string perthite and patch perthite are recognizable, but none of the perthitic intergrowths shows regularity of form or orientation. A few grains of orthoclase in the graphic intergrowth are clear and are free from albite lamellae.

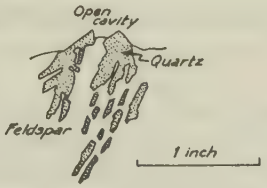


FIG. 3. Graphic texture in druse wall.

The fine-grained graphic intergrowth of this perthitic orthoclase with quartz is the universal enclosing material of the druses. The intergrowth near the druses in some cases shows a flamboyant structure perpendicular to the walls of the cavities (Fig. 3). Near the druse walls albite may take the place of orthoclase in the graphic intergrowth.

In addition to the micro-perthitic orthoclase of the graphic intergrowth, there are in several specimens large orthoclase crystals projecting from the walls into the open cavities. This euhedral orthoclase appears to be continuous with that of the graphic intergrowth. The orthoclase crystals (in one instance a complete Carlsbad twin) are pink or yellowish in color, are coated with later minerals, especially the chlorites, and are associated with crystalline albite and smoky or white quartz crystals. These minerals are evidently later than the orthoclase, and in some instances the albite has clearly attacked orthoclase by replacement. Some of the euhedral orthoclase shows "mutual" relations with albite, indicating a probable contemporaneous formation of the latest orthoclase and

the earliest albite. Some of this euhedral orthoclase is perthitic, but it is not certain that the larger latest orthoclase crystals contain micro-perthite lamellae because there are no thin sections which cut them. In any case, neither thin sections nor hand specimens indicate any break in deposition between the orthoclase of the graphic intergrowth and the crystalline orthoclase of the druses.

*Oligoclase and andesine*

A few grains of oligoclase were observed completely enclosed in microperthitic orthoclase. Determination of the mineral in thin section indicated oligoclase containing 18% An. These grains were probably derived from the surrounding rock and incorporated in the pegmatite material: they do not appear to form part of the pegmatite texture.

A little andesine was also seen in thin section. It was found in graphic intergrowth with quartz in the same manner as the microperthitic orthoclase. The origin of the andesine, found only in a single thin section, is doubtful. It may be a replacement of orthoclase in the intergrowth, or it may be of the same age as orthoclase and quartz.

*Quartz*

There are three modes of occurrence of quartz in the Striegau specimens: (1) quartz in graphic intergrowth with feldspar, forming the pegmatite material surrounding the druses; (2) white, crystalline quartz on the druse walls and projecting into the open cavities; (3) crystalline smoky quartz in the druses projecting into open space. The first two types grade directly into each other; the smoky quartz appears to belong to a distinct and later period of mineralization, but it is contemporaneous with some of the white quartz (Fig. 4).

Most of the quartz of the graphic intergrowth is contemporaneous with the associated orthoclase, although some of the quartz is earlier, as shown by perthitic potash feldspar filling cracks in quartz.

Quartz deposition continued without a break into the period of albitization to form the crystalline white quartz. This white quartz is either intergrown with contemporaneous albite, or has, in some cases, attacked and covered albite in the druses.

The smoky quartz is associated with albite (cleavelandite), grows on albite in some instances, and covers or encloses large orthoclase crystals. The smoky quartz forms the largest of the quartz crystals.

All of the quartz is coated in the druses by younger minerals, especially chlorite, epidote, and zeolites.

*Albite*

Albite is found in these specimens as (1) perthite lamellae in potash feldspar; (2) in graphic intergrowth with quartz near the druse walls; (3) as coarse white crystals (cleavelandite) lining the druses. It is apparent that albitization is a distinct stage of mineral deposition.

There is evidence in hand specimen and in thin section that albite is replacing orthoclase. In one section albite with perthitic potash feldspar cores was observed. The albite which is in graphic intergrowth with quartz apparently gives way to orthoclase at a distance from the druses, and is probably, therefore, a replacement of the graphic orthoclase in the main part of the pegmatite. The cleavelandite deposition continued after cessation of potash feldspar formation, and cleavelandite covers orthoclase in the druses. It is reasonable, on the basis of this extensive albitization, to consider the irregular, microscopic, string perthite and patch perthite lamellae of albite in potash feldspar as being also the result of replacement, although Schwantke (1896, pp. 70, 77–79) believes that the perthitic albite is contemporaneous with the graphic potash feldspar.

The coarse crystalline albite on the druse walls, resting on fine-grained graphic orthoclase, illustrates the most prominent mode of occurrence of the mineral. The albite is in some instances in comb-like forms, the result of the combination of {001} and {101}, as Schwantke (1896, p. 32) has previously observed. The albite of the druse walls is closely associated with contemporaneous white, crystalline quartz and with large smoky quartz crystals. Some of the smoky quartz crystals grow on albite. Albite also forms a base for chlorite, epidote, zeolites, and calcite.

*Magnetite*

A few fairly large irregular grains of magnetite bordered by biotite and chlorite were seen in thin section associated with albite and quartz. The exact paragenetic position of the magnetite is doubtful. It was not seen in hand specimen.

*Sphalerite*

One individual of sphalerite was observed. The sphalerite, associated with biotite, was perched on quartz and albite.

*Chlorite* (*strigovite, prochlorite, penninite*)

The principal mode of occurrence of the chlorite minerals, of which the three named above were identified, is as a thin coating on earlier quartz and feldspars. Where the chlorite coating has formed on quartz, the chlorite coats selectively the prism faces rather than the pyramid. The chlorite coating may also form a layer separating albite from zeolites and

calcite, and chlorite commonly forms a base for bunches of epidote prisms.

The chlorite minerals are also found in cracks in the quartz and feldspar of the druse walls.

Of the three chlorite minerals identified, strigovite and prochlorite are the most abundant. The strigovite is found in formless, fine-grained, dark green masses and coatings. The prochlorite is in very small green flakes, intimately associated with strigovite. Penninite, identified in only one specimen, is in fairly large mica-like flakes of pale green color, associated with the other chlorites. Tourmaline needles grow on the penninite.

*Tourmaline*

Tourmaline is rare in the specimens. It was observed in very thin, hair-like, colorless needles and fibres growing on chlorite. Many of the tourmaline needles are enclosed in later stilbite, and the tourmaline can be seen extending through the transparent stilbite and protruding from opposite sides of the stilbite crystal.

The indices of the tourmaline show that the mineral contains a considerable proportion of lithium and manganese.

*Fluorite*

Fluorite is found in scattered small crystals, isolated and growing on quartz, feldspar, or chlorite, or in open cracks in quartz or feldspar. The mineral is pale violet in color. Epidote prisms of younger age grow against and around many of the fluorite crystals.

*Muscovite*

Muscovite, chiefly as sericite, is of very rare occurrence. It was observed in thin section associated with epidote and replacing potash feldspar.

*Molybdenite*

In a single specimen a fairly large bunch of radially arranged sheets and flakes of molybdenite can be seen on chlorite which is coating feldspar and quartz. Stilbite has formed on some of the molybdenite.

*Epidote and clinozoisite*

Epidote and clinozoisite together are, with chlorite, the most abundant minerals of the later druse-filling stage. Epidote is found as beautiful bunches and reticulating networks of slender apple-green prisms on the walls of the cavities. Clinozoisite grows in the same manner, but it is pale gray-green in color. There are evidently all gradations from normal epidote to clinozoisite containing up to 7% of the iron-epidote molecule.

These minerals are commonly found on chlorite and are associated with later interstitial stilbite. Epidote and clinozoisite have also grown on other earlier minerals, chiefly albite, quartz, and fluorite. In thin section epidote was observed extending along cleavage planes of biotite and chlorite, and in cracks in quartz and feldspar.

*Axinite*

Axinite is the last mineral deposited in the later druse-filling stage. It is found in well-formed, clear, tan-colored crystals on chlorite, albite, or euhedral orthoclase. Stilbite may be seen perched on axinite.

*Heulandite*

Although the succession of the zeolites is not clearly defined, heulandite appears to be the earliest. It was identified with certainty only in one specimen, where it can be seen in fairly large (up to 3 mm.), pale, yellow-brown crystals exhibiting perfect {010} cleavage and the characteristic opalescent luster.

Heulandite has grown on epidote and feldspar, and it is evidently earlier than stilbite, which rests upon the heulandite.

*Stilbite (and epidesmine)*

Stilbite is the most abundant of the zeolites, and is found in nearly every specimen. It grows in characteristic tufts and bunches of straw-yellow prisms in open spaces in the druses, perched upon various earlier minerals, especially smoky quartz, feldspar, and chlorite. Stilbite may be seen in abundance in the openings between reticulating epidote prisms.

Microscopic study of some very pale-colored crystals having the appearance of stilbite indicated that they are probably the orthorhombic mineral epidesmine. Different investigators, however, do not agree exactly as to the properties of epidesmine.

*Laumontite (caporcianite)*

Laumontite was observed in bunches of tiny white needles associated with earlier epidote crystals and growing on chlorite. The indices of the mineral indicate the variety caporcianite, an alteration product which has lost about 18% of its original water content.

*Chabazite*

Red chabazite is found in several of the specimens in small characteristic psuedo-cubes (i.e., rhombohedrons). The mineral grows on quartz, clinozoisite, or chlorite. In one specimen the red chabazite is embedded in younger crystalline calcite.

*Calcite*

Calcite apparently represents a final stage of mineral deposition in the druses. It is found as colorless or flesh-colored crystals in open spaces and coating earlier minerals. It is definitely younger than stilbite and chabazite. It may be found growing also on smoky quartz, feldspar, and chlorite. In one specimen there is a layer of calcite crystals (maximum diameter 1 cm.) having the hexagonal form resulting from the combination of the prism and the basal pinacoid. This layer of calcite is separated from albite by a band of chlorite.

*Limonite*

A little limonite was seen forming a botryoidal black coating on quartz, feldspar, and zeolites. This is evidently of very late origin, probably resulting from the action of meteoric waters percolating into the cavities.

*Manganese oxide*

A dull black coating on albite and epidote is apparently manganese oxide. The origin is probably similar to that of the limonite.

## Discussion of Mineral Paragenesis

The paragenetic sequence of the Striegau minerals, as presented here, is the result of the study of a relatively small number of specimens and thin sections. All of the specimens consist of parts of the lining of open druses in the pegmatites. The age relations determined are presented diagrammatically in Fig. 4. The diagram is not intended to imply the inflexibility which it seems to express, but it is believed that the general sequence, the depositional ranges, and the mineralization stages are in a general way correct.

*I. Magmatic stage of mineral formation*

This stage represents the earliest period of pegmatite formation. During this stage the main pegmatite bodies were produced, and, in the specimens studied, the minerals of this period are found as the fine-grained graphic quartz and feldspar intergrowth surrounding the druses. Potash feldspar and quartz are dominant and are evidently of simultaneous deposition. They are associated with some interstitial biotite, a little andesine, some other plagioclase derived from the surrounding rock, and perhaps a little albite of contemporaneous age. Toward the end of this period and in the beginning of the following period of albitization, the magmatic solutions were of such a character as to dissolve out part of the previously formed pegmatite material, leaving the druses in which

the later pegmatite minerals were deposited. The character of the solutions which produced the druses cannot be determined. In some instances, however, the formation of potash feldspar was able to continue and to develop the relatively large orthoclase crystals found on some of

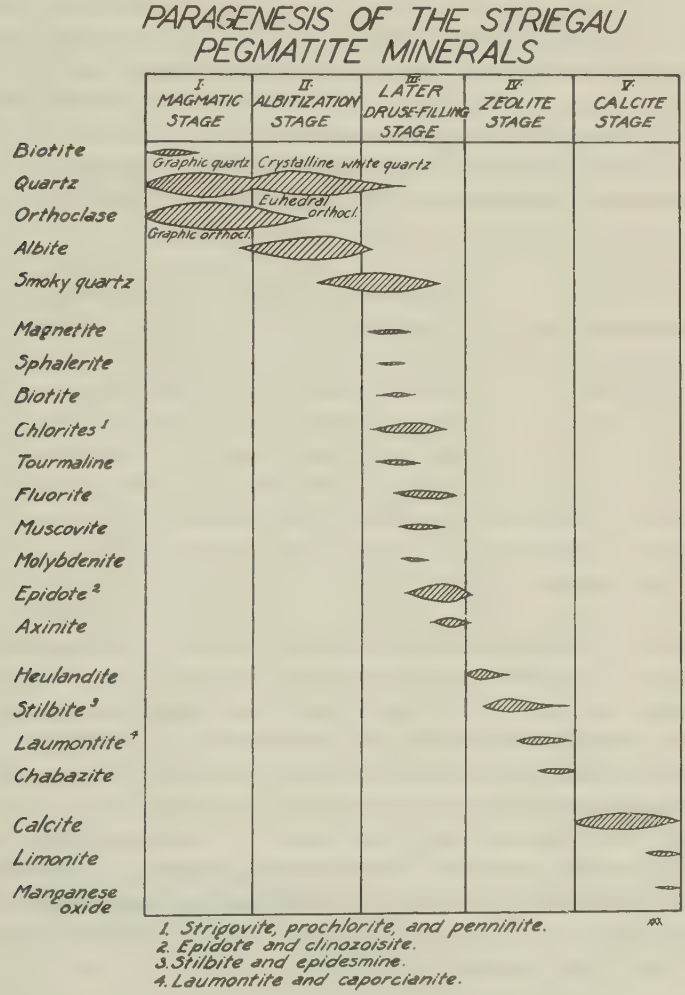


FIG. 4

the druse walls. The specimens do not show, except in coarseness of grain and better crystalline development, any marked difference or evidence of depositional break between the potash feldspar of the graphic intergrowth and the orthoclase crystals on the druse walls.

Silica mineralization continued through this and the next stage without interruption.

*II. Albitization stage*

The beginning of this stage of mineralization, although probably not separated by any cessation of deposition from the magmatic stage, is marked by the formation on the druse walls of coarse-grained albite and cleavelandite. Albite in continuation with this is found in graphic intergrowth with quartz next to many of the druses and, as far as it is possible to deduce from the small specimens available, albite gives way to potash feldspar (which is in graphic intergrowth with quartz) at greater distance from the druses. It can be seen in some hand specimens that albite apparently attacked and replaced potash feldspar crystals in the walls of the cavities.

It seems, therefore, that the formation of albite represents a later stage than the magmatic one, although not separated by a depositional break, and that a change in the character of solutions, perhaps the same change which caused the formation of the open spaces, resulted in crystallization of cleavelandite in the druses and even caused replacement by albite of some of the potash feldspar of the druse walls. The possibility is suggested that the micro-perthitic albite lamellae in the potash feldspar are also the result of replacement during the albitization stage.

Schwantke (1896, pp. 70, 75–76, 77–80), however, considers albite as part of the magmatic stage of deposition, at first contemporaneous with quartz and orthoclase, but continuing after cessation of potash feldspar deposition. He considers the perthite to be definitely the result of contemporaneous deposition of orthoclase and albite. It is obvious that, if Schwantke's idea of the continuation of albite deposition after the formation of potash feldspar be given prominence, his concept and that presented here are not greatly at variance, except that Schwantke does not recognize replacement by albite.

During the albitization stage silica deposition continued, and the white crystalline quartz associated with coarse albite in the druse walls was formed. White quartz deposition also continued into the succeeding mineralization stage. Toward the end of the period of albitization large crystals of smoky quartz were formed.

*III. Later druse-filling stage*

A distinct break between depositional stages apparently occurred at the close of the albitization stage. After cessation of the abundant albite deposition, the character and quantity of the minerals changed radically.

During this later druse-filling stage minerals were deposited in relatively small quantities, but they contain a great variety of elements. The minerals of this period are found in many cases in cracks in the druse walls and in the earlier-formed minerals. This indicates a possible period of contraction and consequent fracturing at the close of albite mineralization.

The paragenetic positions of magnetite, sphalerite, and biotite are doubtful because they are found only in very small amounts and are isolated. Chlorites (strigovite, prochlorite, and penninite) are important in this stage, and are early in the sequence. They coat earlier-formed quartz and feldspar. Tourmaline and fluorite are indications of some possible pneumatolytic action. Epidote and clinozoisite are important toward the close of this stage, and probably indicate hydrothermal action following pneumatolysis. Schwantke (1896, pp. 81–82) believes that the epidote was formed by the action of thermal waters on potash feldspar, on biotite (the source of the iron), and on plagioclase from the surrounding rocks (source of the CaO). Axinite is the only mineral of this stage which is later than epidote, and may also represent hydrothermal action, the waters bringing into the druses some of the material previously deposited by pneumatolytic solutions (Schwantke, 1896, p. 82).

The minerals of this stage of deposition are found principally as crustifications, bunches of needles, or as isolated grains resting on the older minerals in the cavities and in open cracks in these minerals.

*IV. Zeolite stage*

The introduction of zeolites marks another distinct stage of mineralization, and there may well have been an appreciable time interval following the later druse-filling stage before zeolite deposition commenced. Schwantke (1896, p. 83) finds prehnite as the earliest mineral of the zeolite stage, and believes that this mineral forms a gradation between the two mineralizing periods. However, no prehnite was recognized in the specimens studied here.

It is difficult to establish a sequence of deposition for the various zeolites from the specimens at hand because a single specimen rarely contains more than one or two zeolites. The sequence shown in Fig. 4 is thought to be as accurate as possible for the material studied. Stilbite is decidedly more abundant than the other zeolites.

The late deposition of the zeolites as a whole is clearly shown: these minerals are found perched on the surfaces of minerals of the preceding stages in hollows and open spaces. They probably represent the final waning action of cooling thermal waters.

*V. Calcite stage*

Calcite alone is the representative of a final mineralization period, and is the result either of the action of meteoric waters or of carbonate-bearing hydrothermal solutions. Crystalline calcite is found in considerable abundance in certain of the druses, and it is definitely younger than the zeolites.

Schwantke (1896, pp. 83–85) quotes Websky as believing that the calcite represents the remains of blocks of limestone which were caught up in the pegmatite material. Websky explains many of the druses as having been formed by the dissolving out of these limestone fragments. Schwantke considers it possible that the druses were once completely filled with calcite, much of which has been removed in solution, but he finds in the plagioclase of the granite the probable source of the calcium carbonate, and he sees no evidence of the contact minerals which would be expected in the druse walls if limestone fragments had been engulfed in the magmatic material. Gürich (1920, p. 310) also is of the opinion that the druses were once entirely filled with calcite, but he thinks that the deposition of calcium carbonate was part of the magmatic process, and that the calcite material was derived neither from limestone fragments nor from the plagioclase of the granite.

Actually there is no positive evidence for a former complete filling of the druses by calcite, and there certainly is no support for the limestone fragment idea. The source of the calcium carbonate is a matter of question, and it is equally difficult to decide whether meteoric or hydrothermal waters are responsible for calcite deposition.

## Summary

Within a granite mass at Striegau, Silesia, are vein-like and horizontal sheet-like pegmatite bodies. The pegmatites consist largely of feldspar and quartz, feldspar being by far the most abundant mineral. The pegmatites contain a great number of open druses in which were deposited most of the minerals discussed here.

During the first, or magmatic, stage of mineral formation the main pegmatite bodies were produced. The fine-grained graphic intergrowth of quartz and potash feldspar forming the druse walls belongs to this period. Deposition of quartz and orthoclase continued into the second, or albitization, stage. Coarse-grained albite and cleavelandite lining the druses are characteristic minerals of this stage. The albite evidently replaced some of the potash feldspar. The formation of the open cavities is to be assigned to the early part of the albitization period.

A distinct break marks the end of the albitization stage, which was succeeded by a second period of druse filling. The minerals of this stage include chlorite (strigovite, prochlorite, and penninite), tourmaline, fluorite, epidote, clinozoisite, and axinite. These minerals are found in relatively small amounts as crustifications and isolated crystals perched on the earlier minerals which line the cavities. Pneumatolytic and hydrothermal action are indicated.

Another distinct stage of mineralization is represented by zeolites, principally stilbite. These minerals were probably deposited in the druses during the waning action of cooling thermal solutions.

Calcite in the cavities is representative of a final mineralization period and is the result of deposition either from meteoric waters or from carbonate-bearing hydrothermal solutions.

## Acknowledgments

The writer wishes to acknowledge the assistance of Professor Charles Palache during the course of the work. Thanks are also due to Dr. Cornelius S. Hurlbut, Jr., for criticism of the manuscript.

The study is based upon a group of Striegau specimens in the Mineral Collections of Harvard University.

## References

Gürich, G., Zur Geologie der Striegauer und Jenkauer Berge. Abstract and review in *Neues Jb. Min.*, 309–313 (**1920**); original in *Jb. d. preuss. geol. Landesanst.*, **36,** Heft 2, part 3, 595–622 (1915).

Schwantke, A., Die Drusenmineralien des Striegauer Granits (Leipzig, **1896**).

Von Bubnoff, S., Geologie von Europa, **2,** part 1, 538–539; 550 (1930); in *Geologie der Erde* series (Berlin).

# PROGRESSIVE METASOMATISM OF SERPENTINE IN THE SIERRA NEVADA OF CALIFORNIA

GORDON A. MACDONALD, *333 Federal Bldg., Honolulu.*

ABSTRACT

Nodules of serpentine enclosed in mica schist close to a body of intrusive quartz diorite have been altered by igneous emanations. Cores of residual serpentine are surrounded by successive envelopes of talc, talc and actinolite, actinolite, chlorite, and biotite. In some, veinlets of biotite transect the entire nodule. Chemical and micrographic analyses indicate that the changes involved the loss of magnesia from the nodules, the addition of silica in the inner zones, and the addition of small amounts of other oxides in the outer zones. The process of alteration resembled that often designated as granitization, but because of the extremely mafic composition of the original rock, the products have no similarity to a granitic rock.

## INTRODUCTION

In the northwestern part of the Dinuba quadrangle, in the western foothills of the Sierra Nevada between the Kings and the San Joaquin rivers, California, serpentine nodules enclosed in mica schist have been altered by emanations from an adjacent body of quartz diorite with resultant formation of a group of new minerals arranged concentrically about residuals of the original rock. Typically, a core of serpentine is surrounded by talc, which passes outward into a zone of admixed talc and actinolite, and finally into a zone of nearly pure actinolite. The actinolite in turn is surrounded by a rim of biotite, and the whole is embedded in a matrix of biotite schist. The occurrence is closely similar to others on the island of Unst in the Shetland Islands, described by H. H. Read.[1]

The nodules are exposed for only a few tens of feet in a road-cut just west of the store at Humphreys, in section 22, T 11 S, R 23 E, Mount Diablo Base and Meridian. They were discovered by Professor Howel Williams and a class in field geology from the University of California, and have been studied by the writer in connection with an investigation of the geology of the surrounding region. At the time the locality was first visited by the writer, the surface of the cut was heavily masked by soil and debris from the bank above, but violent rains during the spring of 1938 washed away much of the concealing soil and exposed the bedrock. Succeeding collecting expeditions by classes from the University of California have nearly exhausted the locality.[2]

The writer wishes to thank Dr. Howel Williams of the University of California, and Dr. Cordell Durrell of the University of California at Los Angeles, both of whom read and criticized the manuscript of this paper, and Mr. James Y. Nitta, who prepared the illustrations.

[1] Read, H. H., On zoned associations of antigorite, talc, actinolite, chlorite, and biotite in Unst, Shetland Islands: *Min. Mag.*, **23**, 519–540 (1934).

[2] Williams, H., personal communication, May 1940.

## Geologic Setting

The Bedrock Complex of the western Sierra Nevada in the vicinity of the Kings and San Joaquin rivers consists of a series of metamorphosed sedimentary and volcanic rocks intruded by the granitic rocks of the

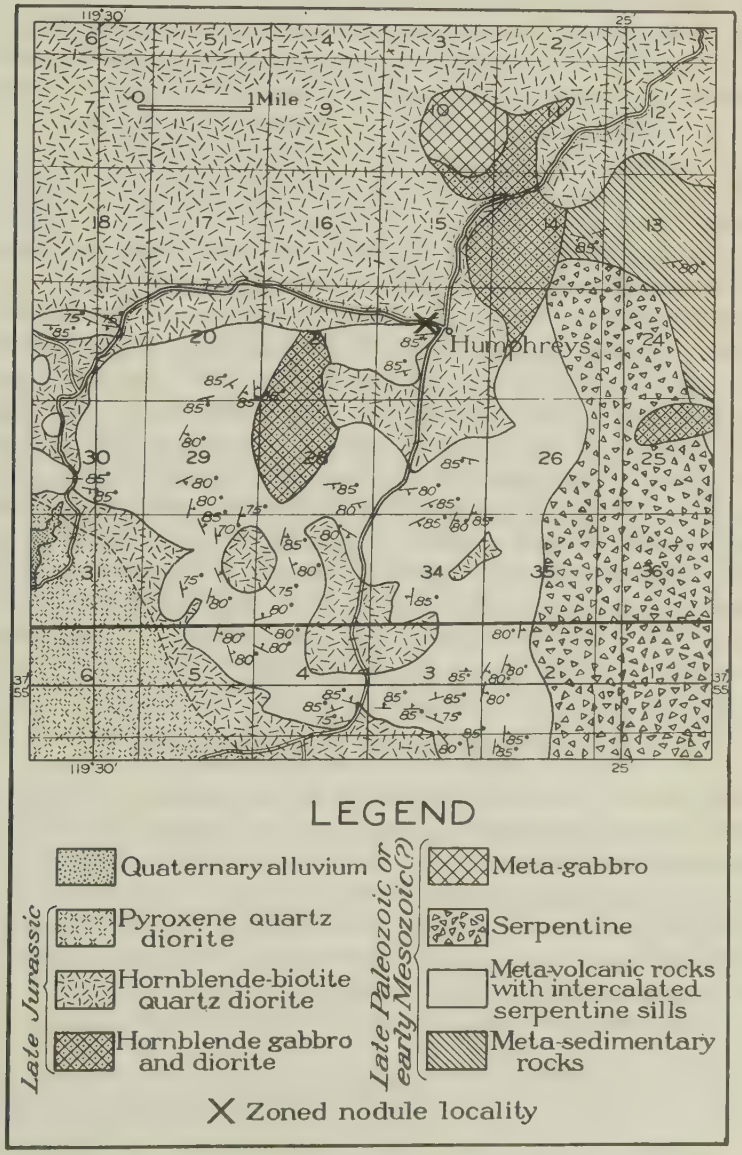


Fig. 1. Geologic map of the northwestern part of the Dinuba quadrangle, Calif.

Sierra Nevada composite batholith. The sediments and volcanic rocks were accumulated probably during late Paleozoic and early Mesozoic time in the sinking Sierra Nevada geosyncline, and during the geosynclinal period they were intruded by numerous sills of serpentine. These serpentine bodies have undergone the same degree and type of metamorphism as the enclosing rocks.[3] Accompanying the intrusion of the Sierra Nevada batholith there was widespread granitization along contacts, resulting in the production of extensive areas of injection gneisses, as well as other more local effects. The alteration of serpentine described herein is merely one local result of this widespread granitization.

The accompanying map (Fig. 1) shows the position of the zoned nodule locality in relation to the general geology of the surrounding region. The serpentine body from which the nodules were derived is a narrow sill lying between biotite schist and plagioclase amphibolite. The granitic intrusion which followed the folding removed part of the enclosing rocks, so that the sill now lies near the northern edge of a roof pendant which continues westward for about twelve miles through the Academy and Friant quadrangles. This roof pendant is made up very largely of plagioclase amphibolites, with lesser amounts of interbedded metasedimentary rocks. Several narrow sills of serpentine are present, and these have been extensively altered by igneous emanations to talc or talc-tremolite schists.

The quartz diorite of the batholith is in contact with the mica schist, along the other margin of which was intruded the serpentine sill from which the zoned nodules were derived. The actual contact of the quartz diorite with the mica schist is not exposed, but the thickness of the schist cannot be more than 50 feet, and is probably less. The attitudes in the metamorphic rocks are nearly vertical, and the quartz diorite contact dips under the mica schist at a high angle.

## Description of the Nodules

The zoned nodules are embedded in the mica schist between the serpentine sill and the margin of the batholith. They range in diameter from about 10 cm. to over a meter. In shape they vary from nearly spherical to much flattened ellipsoids. When it was well exposed, the roadcut had somewhat the appearance of pillow lava, the nodules standing out in relief from the less resistant biotite schist matrix. The entire mass is cut by narrow dikes of aplite and pegmatite, and by a few quartz veins.

All of the larger nodules, and many of the smaller ones, contain a core

[3] Durrell, C., Metamorphism in the southwestern Sierra Nevada northeast of Visalia, Calif.: *Univ. Calif. Publ., Bull. Dept. Geol. Sci.*, **25,** 15 (1940). Macdonald, G. A., Geology of the western part of the Sierra Nevada between the Kings and San Joaquin rivers, Calif.: *Univ. Calif. Publ., Bull. Dept. Geol. Sci.*, in press.

of massive, dark grayish-green serpentine, and in general the size of the core increases with the size of the nodule. The core is sharply separated from an enclosing zone with radial fibrous structure composed of varying amounts of talc and actinolite. The thickness of this radial zone ranges from about 1 to 20 cm., and has little relation to the size of the nodule. In many of the smaller nodules the serpentine core is absent and the talc-actinolite zone extends to the center. Conversely, in the largest nodules the serpentine core may be $\frac{1}{2}$ to 1 meter in diameter but the radial zone still only a few centimeters thick. The radial zone is in turn surrounded by a massive zone, of very variable thickness, composed almost entirely of actinolite. In places this zone attains a thickness of a little over $2\frac{1}{2}$ cm., but elsewhere it is entirely absent. The boundary between this zone and the radial zone appears quite sharp in the hand specimen. Also sharply separated from the actinolite zone is the outer envelope of biotite. This too is of variable thickness, ranging from a mere film to over 2 cm. in cross-section. It is made up almost entirely of flakes of brown biotite oriented parallel to the margin of the nodule. The biotite rim passes gradationally outward into a matrix of biotite schist. In some nodules veinlets of brown biotite lead inward from the biotite rim across the actinolite zone and the radial talc-actinolite zone, and in a few instances they transect the entire nodule (Fig. 2-B). These veins pinch and swell from a mere film to as much as a centimeter in thickness. A chlorite zone situated between the actinolite and biotite zones, such as is found in some of the Unst occurrences,[4] is present only in rare instances. Chlorite is found in small amounts throughout the nodules, even in the serpentine cores, but generally does not form any definite zone.

One specimen, typical of the completely developed nodules of intermediate size, approaches in shape a triaxial ellipsoid, with diameters of 19 cm., 16 cm., and 12 cm. The serpentine core is very small, its cross-section along the plane of the major and minor axes of the ellipsoid measuring only 1.2 cm. by 2.5 cm. It is surrounded by a zone with pronounced radial structure measuring in the same plane 3.7 cm., by 7.5 cm. This radial zone consists of an inner band about 7 mm. thick composed almost entirely of talc, and an outer band composed of a mixture of talc and actinolite in varying proportions. This latter band is light green in color, and within it lie dark green radial streaks consisting almost entirely of actinolite. Surrounding the radial zone is a zone of dark green actinolite in which the prismatic crystals show haphazard orientation. In places this actinolite zone is absent, but in other places it reaches a thickness of 1.5 cm. Completely surrounding the entire nodule is an envelope of biotite ranging from a thin film to about 7 mm. thick.

[4] Read, H. H., *op. cit.*, pp. 526, 529.

Another specimen is slightly smaller, and the serpentine core is absent. The dimensions of the nodule are 17 cm., by 15 cm., by 8 cm. It consists very largely of the radial talc-actinolite zone, which is surrounded by a zone of actinolite ranging in thickness from 0 to 1.2 cm., and this in turn is surrounded by an outer layer of biotite 1 to 10 mm. thick. Veinlets of biotite transect the entire nodule.

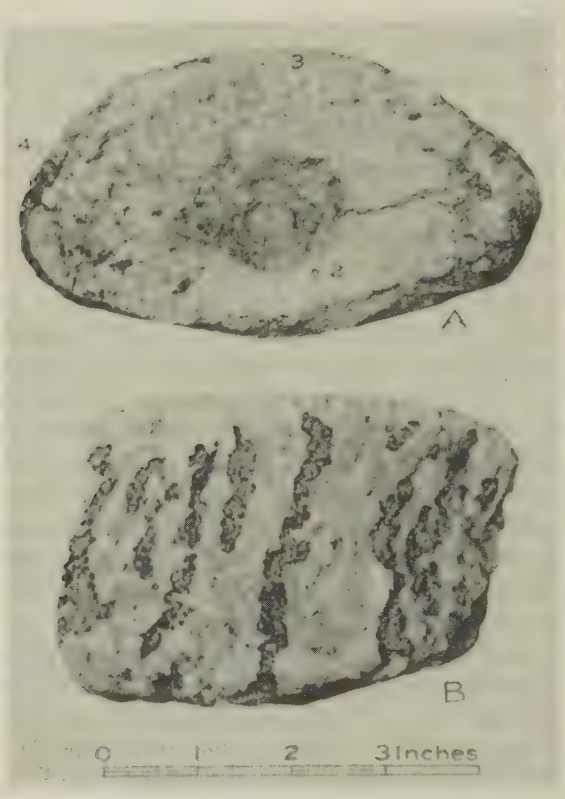


FIG. 2. *A*. Cross-section of a zoned nodule showing the serpentine core (1) surrounded by the radial talc-actinolite zone (2), the actinolite zone (3), and the biotite rim (4). Dark spots in the radial zone are nests of biotite.

*B*. Nodule with edges broken away to expose the talc-actinolite zone, crossed by dark veinlets of biotite.

*The serpentine core.* In thin section the serpentine of the cores is composed predominantly of web-structure antigorite, polarizing in light gray colors, the small length-slow fibers showing a criss-cross orientation like the warp and woof in woven cloth. Scattered throughout this matrix are grains of a rhombic pyroxene, forming irregular frayed-appearing patches as much as 3 mm. across, which evidently represent relict grains of the

original peridotite, spared by the serpentinization and by the dynamothermal metamorphism which produced the web-structure antigorite. These grains are pale brown, non-pleochroic, and are cut by many small veinlets of the antigorite and also by rows of small grains of regenerated olivine. The pyroxene has an optic angle near 90°. Tiny subhedral to anhedral grains of iron ore are scattered abundantly through the pyroxene. Small subhedral to anhedral grains of colorless olivine are distributed throughout the rock, embedded in the antigorite and also in the pyroxenes. Some grains of pyroxene are almost completely replaced by small grains of olivine, the outline and structure of the original pyroxene grain being still visible. The olivine has an optic angle close to 90°. It is evident from its relationships that it represents regenerated metamorphic olivine, like that described elsewhere.[5]

Scattered throughout the antigorite groundweb are small, subhedral to anhedral flakes and tablets of an ultra-brown polarizing chlorite, which shows a (+) $2V$ of about 10°, and negative elongation, the acute bisectrix $Z$ emerging approximately normal to the basal cleavage. Its dispersion is $r<v$ weak. The mineral may be a positive penninite, but except for its lower birefringence, its properties correspond with those of the clinochlore which is a common constituent of the contact metamorphosed serpentines of the Sierra Nevada.[6] Associated with this in a few places are small flakes of an ultra-blue polarizing chlorite with positive elongation, which is probably penninite. Talc is present locally as tiny flakes and shreds between the fibers of antigorite. Anhedral grains of iron ore, opaque in transmitted light and metallic gray in reflected light, are scattered abundantly throughout the rock.

*The talc zone.* A thin section cut from the talc zone is intermediate in composition between the talc-actinolite zone and the serpentine core, being composed largely of talc and serpentine, with talc about twice as abundant as serpentine. Chlorite, polarizing in both ultra-brown and ultra-blue colors, is also fairly abundant. Ore minerals are found as scattered small grains throughout most of the rock but certain small irregular areas are composed almost wholly of ores and chlorite. In some of these areas the two minerals are present in nearly equal amounts, but chlorite is usually considerably the more abundant. In one place a few flakes of brown biotite ($-2V=0°$) are associated with talc and serpentine.

*The talc-actinolite zone.* A section cut across the inner part of the talc-actinolite zone consists largely of a felty aggregate of talc, in which lie needles of actinolite. The actinolite, which forms about 5 per cent of the rock, shows the following properties: colorless, with a very large negative

[5] Durrell, C., *op. cit.*, p. 82. Macdonald, G. A., *op. cit.*

[6] Durrell, C., *op. cit.*, p. 84.

optic angle, an extinction angle $Z \wedge c$ of 18°, and birefringence moderate, about .025. The talc appears uniaxial, with a negative sign. The individual grains composing the aggregate of talc are xenoblastic and often highly irregular. The actinolite is hypidioblastic in the prism zone, but terminal faces are lacking. A few small flakes of chlorite are present, and grains of iron ore are scattered throughout the slide. The iron ore grains are for the most part hypidioblastic, and more or less square in outline, and often contain small inclusions of talc. The presence of a small amount of brown picotite associated with some grains indicates that they are probably chromite, but others may be magnetite.

Another section, from the middle of the talc-actinolite zone, is very similar to that just described, except that actinolite forms about 40 per cent of the rock.

A thin section from the outer part of the radial zone of the specimen analyzed (see accompanying table) is composed largely of long blades of actinolite, idioblastic in the prism zone but lacking terminal faces, with a large negative optic angle and $\gamma = 1.646$ ($\pm .003$). Between them lie xenoblastic grains of talc. A small amount of chlorite is present as anhedral grains, pleochroic from $X$ = pale yellow to $Y$ and $Z$ = pale yellowish-green. It appears uniaxial, with $X$ nearly normal to the basal cleavage. Irregular granules of iron ore are scattered throughout the rock, and associated with some grains are small amounts of a brown isotropic mineral with a high index of refraction, probably picotite.

A Rosiwal microscopic analysis of a strip across the section at right angles to the radial structure yields the following results in per cent by area:

| | |
|---|---|
| Actinolite | 89.1% |
| Talc | 7.9 |
| Chlorite | 2.6 |
| Ore | 0.4 |

Sections through the actinolite zone are made up very largely of hypidioblastic to xenoblastic grains of actinolite, nearly colorless in slides of normal thickness but in thick slides pleochroic with $X$ = very pale yellow, $Y$ = pale yellowish-green, $Z$ = pale bluish-green. Biotite generally makes up about 10 per cent of the rock. It is scattered throughout the slides as irregular anhedral grains. A small amount of talc and chlorite is present in several slides, the chlorite being in many places intergrown with biotite. In some specimens small irregular patches are made up entirely or almost entirely of biotite.

*Biotite zone.* The outermost zone is composed largely of biotite, generally with about 10 per cent of actinolite and a little chlorite. The biotite

shows a small negative optic angle, $\beta = 1.565$ ($\pm .003$), and $X$ = nearly colorless to very pale yellow, $Y$ and $Z$ = yellowish-brown. The analysis of the biotite zone in the accompanying table is of a sample containing about 95 per cent biotite. It shows the mineral to be a phlogopitic variety, low in iron and in alkalies, especially $K_2O$, and fairly high in magnesia.

*Biotite schist.* The mica schist in which the zoned nodules are enclosed is composed largely of brown biotite, with a smaller amount of quartz and a little orthoclase and oligoclase. The biotite occurs in hypidioblastic plates, with their basal planes oriented in parallel position, giving rise to the schistosity. Only a few flakes lie at an angle to the foliation. Between the foliae of biotite lie xenoblastic grains of quartz and feldspar. The schist is distinctly richer in biotite than most of the mica schist of the surrounding region. It is also unusually coarse grained, but in this regard it conforms to the condition generally prevailing in the metamorphic rocks of the district, both the mica schists and the plagioclase amphibolites showing a coarsening of grain near the contacts of the plutonic bodies.

*Quartz diorite.* The adjacent biotite quartz diorite appears normal in every respect, although it has much less hornblende than is typical of the quartz diorites of this region. The texture is granitic. The rock is composed largely of subhedral to anhedral andesine, with abundant albite twinning and rare pericline twinning. Many grains show normal zoning. Anhedral grains of quartz make up about 20 per cent of the rock. Subhedral flakes of biotite, showing slight alteration to chlorite, make up about 10 per cent; it appears to be uniaxial, with a negative sign, $X$ = brownish-yellow, and $Y$ and $Z$ = dark brown. A few grains of pale green hornblende and a few flakes of muscovite are also present. A small amount of orthoclase is interstitial, and zircon and apatite are minor accessories.

## Chemical Composition

Representative specimens of the serpentine core, the outer part of the radial talc-actinolite zone, and the biotite rim have been analyzed. Their chemical compositions are shown in the accompanying table. Column 2 represents the specimen of the talc-actinolite zone of which a Rosiwal analysis has already been given. Assuming the talc to have the composition of the pure mineral, and the chlorite to have the composition of optically similar material found elsewhere in the serpentines of the surrounding district,[7] the approximate composition of the actinolite in this specimen has been calculated. It is shown in column 4 of the table. Using these values the approximate compositions of typical specimens from the

[7] Durrell, C., and Macdonald, G. A., Chlorite veins in serpentine near Kings river, California: *Am. Mineral.*, **24**, 454 (1939).

inner and middle parts of the talc-actinolite zone have then been calculated. The approximate values for the principal oxides thus obtained, together with the same oxides from the analyzed specimens recalculated to 100 per cent, are shown in Fig. 3.

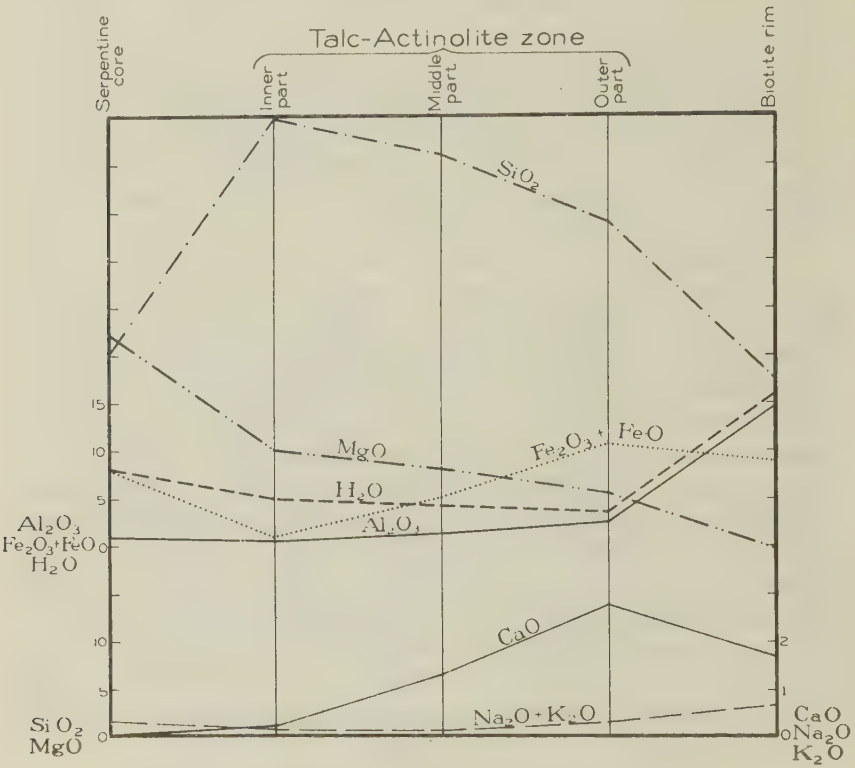


FIG. 3. Graph showing compositions of successive zones in the zoned nodules. The compositions of the inner and middle parts of the talc-actinolite zone were calculated from micrometric analyses; those of the other zones were determined by chemical analyses.

The changes in composition are very similar to those described by Read.[8] The talc zone shows the addition of considerable silica. Magnesia and iron appear to have been removed. The decrease in iron is not definitely proved, since the talc has not been analyzed, but it appears highly probable that at least some decrease in iron, as well as in magnesia, has taken place. The same decrease in percentage of iron is shown in Read's curves.[9] It is possible that some of this apparent loss of iron and magnesia is merely the result of the addition of large volumes of silica, since there is

[8] *Op. cit.*, pp. 533 535.

[9] *Idem*, p. 535.

no evidence that some increase in total volume of the mass has not taken place, but the change in ratio of iron to magnesia clearly indicates migration of one or both of these constituents.

If the decrease in the percentage of iron in the talc zone is considered to be only passive, as a result of the addition of other elements, then there is little or no addition of iron in the outer part of the nodules until the outermost part of the talc-actinolite zone is reached, and there it is only slight. In the outer part of the talc-actinolite zone iron oxide exceeds by only 1 per cent that in the serpentine core.

Other oxides have also been added to the nodules, but in small amounts and to any appreciable degree only in the outer zones. Alumina and lime increase markedly in the outer part of the talc-actinolite zone. Alumina rises still further in the biotite rim, and alkalies show a decided increase. Silica decreases from the talc zone outward, until in the biotite rim its percentage is less than that in the serpentine core. The percentage of magnesia in the biotite rim is less than half that in the serpentine, while the amount of iron is nearly the same.

TABLE 1

| | 1 | 2 | 3 | 4 |
|---|---|---|---|---|
| $SiO_2$ | 40.22 | 54.14 | 37.46 | 55.1 |
| $TiO_2$ | none | 0.19 | 0.87 | — |
| $Al_2O_3$ | 1.49 | 2.52 | 14.64 | 1.8 |
| $Fe_2O_3$ | 4.94 | 3.42 | 7.57 | 3.9 |
| FeO | 2.86 | 7.17 | 1.22 | 8.0 |
| MnO | 0.07 | 0.22 | 0.09 | — |
| MgO | 42.09 | 25.35 | 19.66 | 25.2 |
| CaO | 0.02 | 2.82 | 1.66 | 3.2 |
| $Na_2O$ | 0.21 | 0.19 | 0.53 | 0.2 |
| $K_2O$ | 0.07 | 0.08 | 0.19 | 0.1 |
| $H_2O-$ | 0.07 | 0.07 | 6.89 | 0.04 |
| $H_2O+$ | 7.98 | 3.34 | 8.89 | 3.1 |
| $CO_2$ | none | none | none | — |
| $P_2O_5$ | none | none | 0.06 | — |
| S | none | 0.03 | 0.04 | – |
| $Cr_2O_3$ | 0.14 | 0.28 | 0.07 | — |
| | 100.16 | 99.82 | 99.93 | 100.64 |

1. Serpentine core. Analyst F. A. Gonyer.
2. Outer part of radial talc-actinolite zone. Analyst F. A. Gonyer.
3. Biotite rim. Analyst F. A. Gonyer.
4. Calculated composition of actinolite in outer part of radial zone.

It has been suggested that the migration of the various constituents into the serpentine nodules was in part controlled by the radii of the various ions involved.[10] The greater penetration of silicon in relation to the

[10] Merriam, Richard, unpublished manuscript, 1938.

other elements may be the result of greater ease of diffusion owing to its considerably smaller ionic radius ($Si^{++++}=0.39$Å, in contrast to $Al^{+++}=0.57$Å, $Fe^{+++}=0.67$Å, $Fe^{++}=0.83$Å, $Na^{+}=0.98$Å, $Ca^{++}=1.06$Å, and $K^{+}=1.33$Å[11]). With this exception, however, there appears to be no relationship between the ionic radii and the extent to which the different elements penetrated the serpentine.

## Origin of the Nodules

Small nodular masses of serpentine were in some way separated from the parent serpentine sill and embedded in biotite schist. They may have been small apophyses from the sill which were later sheared off and isolated from the main mass during the Sierra Nevada orogeny. It is also possible that they represent "cold intrusions" of serpentine squeezed into the schist long after consolidation of the sill, in much the same way that masses of serpentine have been squeezed up along fault planes long after solidification in the vicinity of Polonio Pass and elsewhere in the California Coast Range. Masses of serpentine detached from the sill by one means or another would probably migrate readily by plastic flow through the mica schist.

Whatever the method by which they were separated from the parent sill, it is evident that small masses of serpentine enclosed in biotite schist were exposed to the action of permeating emanations from the adjacent quartz diorite. These mineralizers introduced new compounds into the rock, and furthered the recrystallization of the entire system. The process was akin to that of granitization, but because of the extreme composition of the original rock, the product was different from those usually identified as resulting from granitization. The production of amphibolites from limestones by igneous emanations in the Haliburton-Bancroft area in Ontario,[12] and in the Pyrenees[13] is a directly comparable process. Likewise, comparable are the alterations of xenoliths of olivine norite in the Trégastel-Ploumanac'h granite, producing a rock in which the femic minerals are hornblende and biotite,[14] and the similar alteration of holomafic xenoliths in a pegmatite cutting the Dalbeattie granite in Kirkcudbrightshire, England.[15]

[11] Bragg, W. L., *Atomic Structure of Minerals;* Cornell Univ. Press, Ithaca, p. 31 (**1937**).

[12] Adams, F. D., and Barlow, A. E., Geology of the Haliburton and Bancroft areas, Province of Ontario: *Canada Geol. Survey*, Mem. **6** (1910).

[13] Lacroix, A., Le granite des Pyrénées et ses phénomènes de contact: *Services carte géol. France Bull.*, **11,** No. 71 (1900).

[14] Thomas, H. H., and Smith, W. C., Xenoliths of igneous origin in the Trégastel-Ploumanac'h granite, Côtes du Nord, France: *Geol. Soc. London Quart. Jour.*, **88,** 274–296 (1932).

[15] MacGregor, M., A xenolithic pegmatite in the Dalbeattie "granite": *Geol. Mag.*, **73,** 171–184 (1936).

In all of these examples, and particularly in the alteration of the serpentine and limestone, the tendency has been to produce mineral phases in equilibrium with the crystallizing magma, rather than a rock identical with the plutonic rock in composition. This principle was recognized by Lacroix[16] and was clearly stated by Nockolds in his discussion of reciprocal reaction between basic xenoliths and acid magmas.[17]

As a result of his study of the Unst occurrences, Read concluded that the outer edge of the replaced serpentine was at the inner margin of the biotite zone, and that the biotite zone was derived from the enclosing granite gneiss as a result of the migration of magnesia out of the serpentine.[18] This may have been true at the Sierra Nevada locality as well. Indeed, the trend or slope of all of the curves in Fig. 3 except that for the alkalies show a sharp change between the talc-actinolite zone and the biotite rim, supporting the hypothesis that the biotite rim was derived from the enclosing schist rather than from the serpentine. However, the presence of irregular veinlets of biotite penetrating the entire nodules, identical in composition to, and in many places continuous with, the biotite rim, is a conflicting factor. The irregularity of the veinlets, and the fact that frequently nests of biotite are connected with the biotite rim only by minute almost indetectable films of biotite, appear to eliminate the possibility of their having been formed by plastic flow of schist or biotite rim into fractures in the nodule. The biotite veinlets have apparently been formed by metasomatic replacement of the serpentine. Whether the biotite rim was also formed in this way cannot now be definitely decided.

Migration of magnesia out of the altered serpentine nodules probably enriched the surrounding mica schist in that constituent, thus accounting for the greater amount of biotite in the schist at this locality than in most of the mica schists of the district. The greater than usual coarseness of the schist is probably the result of recrystallization in the presence of mineralizers from the adjacent magma.

[16] Lacroix, A., *op. cit.*

[17] Nockolds, S. R., Some theoretical aspects of contamination in acid magmas: *Jour. Geology*, **41**, 571 (1933).

[18] *Op. cit.*, pp. 534–536.

# X-RAY CRYSTALLOGRAPHY OF SHORTITE*

W. E. Richmond,
*U. S. Geological Survey, Washington, D. C.*

Shortite, a double carbonate of sodium and calcium, collected from a drill core 20 miles west of the city of Green River, Sweetwater County, Wyoming, was described by J. J. Fahey (1939). The *x*-ray crystallography was not included in the report because the data had not been obtained at that time.

The following *x*-ray crystallographic data were derived from Weissenberg photographs of a crystal of shortite measuring 1 millimeter in its largest dimension. Rotation, zero and first layer-line photographs were taken about [100]; rotation and zero layer-line photographs about [010]. The lattice constants obtained from these photographs are as follows:

$a_0 = 4.98$ Å
$b_0 = 10.97$ Å
$c_0 = 7.10$ Å

$a_0 : b_0 : c_0 = 0.454 : 1 : 0.647$

The above ratio agrees well with the morphological axial ratio given as: $a:b:c = 0.455:1:0.648$.

The space group was determined from the following reflections to be $D_2^6 - A222$.

$hkl = k+l$ even
$h00 = h$ all present
$0k0 = k$ even
$00l = l$ even

The unit cell content was derived from an analysis by Fahey and a new specific gravity determination made with the Berman balance. The value, 2.60, is lower than the determination, 2.629, made by Fahey with the pycnometer method. In a personal communication Mr. Fahey states that his determination was probably high on account of the presence of included grains of pyrite. The calculated specific gravity, 2.59, agrees well with the lower value. This calculated specific gravity also agrees with the value 2.591 calculated from the specific refractive energies.

| | 1 | 2 | 3 | | | 4 | 5 | 6 |
|---|---|---|---|---|---|---|---|---|
| CaO | 36.34 | 36.64 | 0.653 | 0.654 | | | | |
| MgO | 0.04 | 0.04 | 0.001 | | Ca | 0.654 | 3.996 | 4 |
| $Na_2O$ | 19.91 | 20.07 | 0.324 | | Na | 0.648 | 3.96 | 4 |
| $CO_2$ | 42.90 | 43.25 | 0.983 | | C | 0.983 | 6.01 | 6 |
| Insol. | 0.66 | | | | O | 2.944 | 18.3 | 18 |
| | 99.85 | 100.00 | | | | | | |

Specific gravity 2.60 — Calculated gravity 2.59

* Published by permission of The Director, U. S. Geological Survey.

1. Analysis of shortite from Green River, Sweetwater County, Wyoming; analyst Fahey.
2. Analysis recalculated to 100 per cent.
3. Molecular proportions.
4. Atomic proportions.
5. Number of atoms in the unit cell.
6. Theoretical number of atoms in the unit cell.

The unit cell formula derived from column 5 is $2[Na_2CO_3 \cdot 2CaCO_3]$.

## Reference

Fahey, Joseph J., *Am. Mineral.*, **24**, 514–518 (1939).

## NOTES AND NEWS

### OCCURRENCE OF A COARSELY CRYSTALLINE KAOLIN MINERAL IN SOME SOUTH AFRICAN FIRE-CLAYS

V. L. Bosazza, *University of the Witwatersrand, Johannesburg, South Africa.*

Thin sections of fire-clays almost invariably show shreds and plates of colorless minerals, which although difficult to identify exactly, are almost certainly either dickite or members of the kaolinite-anauxite series. During a visit to a deposit of fire-clay at Boksburg, about 10 miles from Johannesburg, Dr. A. L. du Toit drew my attention to a buff colored clay, which contained "nodules" of an opaline looking material. These "nodules" range up to 1 cm. in length and are sometimes fairly well rounded although more usually somewhat elliptical. The material is flesh colored and easily scratched by a knife.

From one of the larger nodules enough material was removed almost completely free from the surrounding groundmass, for a semi-micro-analysis with the following results.

| | |
|---|---|
| $SiO_2$ | 46.00 |
| $Al_2O_3$ | 36.84 |
| $Fe_2O_3$ | 0.01 |
| $TiO_2$ | trace |
| MnO | nil |
| CaO | not deter. |
| MgO | not deter. |
| Loss on Ignition | 12.58 |
| $H_2O-$ | 5.09 |
| | 100.52 |

*Analyst V. L. B.*

The powder was examined microscopically and found to consist of colorless plates with a low birefringence. The optical properties determined in sodium light are as follows:

$\left.\begin{matrix}\alpha=1.560\\ \beta=1.564\end{matrix}\right\}\pm 0.004$

Biaxial, negative.

Perfect basal cleavage.

The mineral readily adsorbed a deep blue aqueous solution of malachite green, becoming greenish to dark blue in color. The pleochroism was distinct but not very marked. The formula calculated from the chemical analysis corresponds very well to $Al_2O_3 \cdot 2SiO_2 \cdot 2H_2O$ and while the in-

dices are somewhat low it is suggested that the mineral is kaolinite.[1] The immersion oils used were a mixture of a paraffin and alpha-chloronaphthalene.

Thin sections were prepared of this specimen and other non-plastic clays and even more interesting features were noted. Under crossed nicols and *not using conoscopic conditions* an "acute bisectrix figure" is observed. In large elongated grains a series of these figures, sometimes only as single bars, are seen (Fig. 1). These have been described by chem-

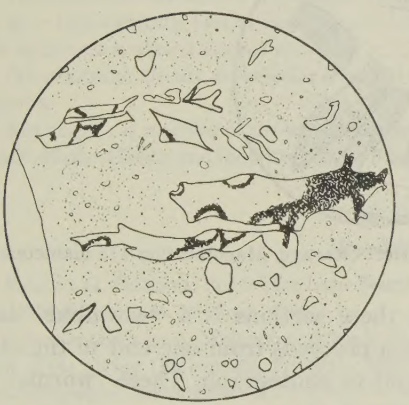

FIG. 1. Non-plastic clay from Boksburg, Transvaal; showing "Extinction Bars." Crossed nicols. Magnification 12 diameters.

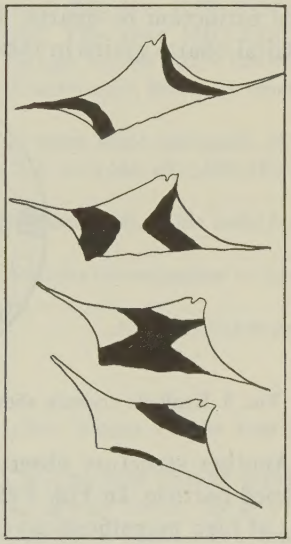

FIG. 2. "Cross of Polarisation" in a shred of kaolinite. Non-plastic fireclay. Magnification 27 diameters. Rotated clockwise.

ists working on fatty acids as "crosses of polarization," but as far as could be traced have not been previously recorded by petrographers. In Fig. 2 the phenomenon in a single shred of kaolinite is depicted diagrammatically. Actually in position 3 the figure is fairly diffuse although fairly sharp in positions 1, 2, and 4. The angle of rotation is about 60°. These dark bars (they are too distinct to be called shadows) are almost certainly due to strain during desiccation of the clay. The clays are hard and compact and do not slake easily on wetting. In thin sections of other fire-

[1] Small amounts of halloysite were unavoidably included in the sample. This mineral was easily distinguished from the kaolinite.

clays this optical effect was also noticed but as the grains are very much smaller, in general being 20–30$\mu$ mean diameter, the phenomenon is not so distinct.

Somers described a spherulite of kaolinite in a white clay which exhibited a similar effect (1). In the present case, however, the strain bars are definitely related to the grain shape. In some slides these kaolinite shreds appeared to have adsorbed some iron, as they are stained fairly uniformly a light brown. In these grains the "strain bars" were observed to be less distinct and cannot be readily distinguished from the undulatory extinction of quartz. It may be noted that none of the rounded detrital quartz grains in these rocks exhibit strain shadows.

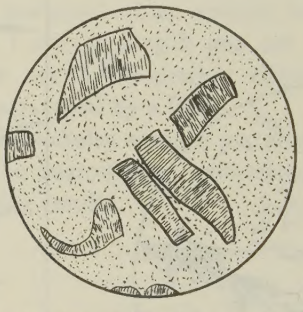

FIG. 3. Kaolinite crystals, showing perfect cleavage. Magnification 175 diameters.

Another structure observed in these sections is a "wormlike" lath-shaped particle. In Fig. 3 extinction proceeds from one end to the other but at high magnifications is difficult to photograph. These "worms" are fairly common in the non-plastic fire-clays.

The replacement of quartz grains by kaolinite is common. However, this may take place in two ways. In one case the replacement is normal as described by Ross and Kerr, and in others the quartz is recrystallized to a very fine grained "cherty texture" (3) intermixed with kaolinite and an anauxite groundmass.

ACKNOWLEDGMENTS

I am indebted to Dr. A. L. du Toit for drawing my attention to this occurrence.

REFERENCES

1. RIES, H., BAYLEY, W. S., AND OTHERS, High grade clays of the eastern United States: *U. S. Geol. Surv., Bull.*, **708**, 314 (1922).
2. ROSS, C. S., AND KERR, P. F., The kaolin minerals: *U. S. Geol. Surv., Prof. Paper*, **165**, 151–176 (1930).
3. BOSAZZA, V. L., A study of the chert of the dolomite series of the Transvaal system: *S. African Jour. Sci.*, **34**, 178–185 (1937).

# NEW MINERAL NAMES

## Kurnakovite

M. N. Godlevsky: Kurnakovite, a new borate. *Compt. Rend.* (Doklady) *Acad. Sci. U.R.S.S.*, **28,** no. 7, 638–640 (1940).

Name: For N. S. Kurnakov, Russian physical chemist.

Crystallographic Properties: Probably monoclinic. Cleavage (010) indistinct. Sections along (001) have pseudohexagonal outlines. Twinning was observed, but the law was not determined. *X*-ray photographs differ from those of other borates and indicate low symmetry.

Chemical Properties: The composition is $Mg_2B_6O_{11} \cdot 13H_2O$, or $2MgO \cdot 3B_2O_3 \cdot 13H_2O$. Analysis by E. N. Egorova: $B_2O_3$ 37.58, MgO 15.46, CaO 0.16, $H_2O$ 47.09, $R_2O_3$ 0.20, $SiO_2$ 0.10, F 0.14; sum 100.73—$(O=F_2)$ 0.06 = 100.67. This gives $MgO:B_2O_3:H_2O = 2:2.81:13.64$, but the figure for $H_2O$ is known to be too high because $B_2O_3$ is lost during dehydration. The mineral is insoluble in water, soluble in warm acids. Before the blowpipe it fuses to an enamel.

Physical and Optical Properties: Found only in dense white aggregates. H. = 3. Sp. gr. = 1.85. Optically biaxial, negative; $\alpha = 1.489, \beta = 1.510, \gamma = 1.525$; all $\pm .002, 2V = 80°$. One optic axis is almost normal to (001).

Occurrence: Occurs as irregular lenses in szaibelyite (ascharite), at the Inder borate deposits.

Relations: A member of the hexaborate group, and similar in composition to inyoite, $2CaO \cdot 3B_2O_3 \cdot 13H_2O$, and inderite, $2MgO \cdot 3B_2O_3 \cdot 15H_2O$.

Michael Fleischer

# NEW DATA

## Penfieldite

Samuel G. Gordon: Penfieldite from Sierra Gorda, Chile. *Notulae Naturae Acad. Nat. Sci. Philadelphia,* no. 69, 8 pp. (**1941**).

A new analysis by A. Meier on crystals from Laurium gave Pb 76.55, Cl 19.82, $H_2O$ 1.59, insol. 0.14; giving the formula $Pb(OH)_2 \cdot 3PbCl_2$, instead of $PbO \cdot 2PbCl_2$. Sp. gr. = 6.61. Crystallographic measurements are given on material from Sierra Gorda, a new locality, and the second one reported for this mineral.

## Herrengrundite Devilline

Heinz Meixner: Die Identität von Herrengrundit (= Urvölgyit) mit Devillin (= Lyellit). *Zentralbl. Min., Geol.*, 244–248 (**1940A**).

Devilline was described by Pisani (*Compt. Rend.*, **59,** 813–814 (1864)) as a copper, calcium sulfate from Lostwithiel, Cornwall. In the same year, Maskelyne (*Chem. News*, **10,** 263 (1864)) gave the name lyellite to material from the same locality, but an analysis was not published until the following year. This analysis by Church (*J. Chem. Soc.*, **18,** 83 (1865)) agrees well with that of Pisani. However, Tschermak (*Ber. Ak. Wien*, **51,** 127 (1865)) examined some of the material and pronounced it a mixture, apparently mostly because when treated with water it gave gypsum and a blue copper sulfate. Meixner has re-examined Tschermak's material, and finds that it is homogeneous and identical with herrengrundite from Herrengrund (or Urvölgy), Slovakia, which was first described in 1879. The pure mineral is decomposed by water as Tschermak described. Meixner suggests that the name herrengrundite be discarded in favor of devilline.

Discussion: Dana (*System*, 6th Ed., **1892,** p. xliii) says, "A name having priority may properly be set aside if it has been lost sight of and has found no one to assert its claim for a period of more than fifty years." Devilline has clear priority, but since the name has not

been used for 75 years, and since the name herrengrundite has been in constant use for over 60 years, it would seem inadvisable to discard herrengrundite and resurrect the name devilline.

M F.

### Tellurobismuthite or Tellurbismuth

CLIFFORD FRONDEL, *Am. J. Sci.*, **238**, 880–888 (1940); preliminary note in *Am. Mineral.*, **24**, no. 12, part 2 (1939).

M. A. PEACOCK, *Univ. Toronto Studies, Geol. Ser.*, no. **44**, p. 67 (1940). Formerly regarded as a sulfur-free variety of tetradymite, $Bi_2Te_2S$, but now considered to be a separate species.

CRYSTALLOGRAPHIC PROPERTIES: Found only as foliated masses or irregular flattened plates. Hexagonal, rhombohedral. *X*-ray data are identical with those given by artificial $Bi_2Te_3$.

$a_0=4.38$, $c_0=30.6$, $a_{rh}=10.51$, $\alpha=24°2'$ (Frondel)
$a_0=4.375$, $c_0=30.39$, $a_{rh}=10.44$, $\alpha=24°11\frac{1}{2}'$ (Peacock).

The rhombohedral unit cell contains $Bi_2Te_3$. Cleavage, basal perfect. Frondel has observed a distinct parting at about 62° to the base.

CHEMICAL PROPERTIES: Composition $Bi_2Te_3$, with only very small amounts of selenium or sulfur.

PHYSICAL PROPERTIES: Laminae flexible, but not elastic. H. = $1\frac{1}{2}$–2. Sp. gr. = 7.81–7.83 (Frondel), 7.80–7.82 (Peacock).

OCCURRENCE: Frondel gives eleven localities, and Peacock two additional. Frequently occurs in intimate intergrowth with tetradymite.

M. F.

## DISCREDITED SPECIES

### Vandiestite

CLIFFORD FRONDEL, *Am. J. Sci.*, **238**, 880–888 (1940).

Vandiestite (also written Von Diestite) was described by Pearce (*Proc. Colo. Sci. Soc.*, **6**, 163 (1902)), as a silver bismuth telluride. Fondel shows that the material is a mixture of tellurobismuthite (see above) and hessite.

### Salvadorite

SAMUEL G. GORDON: The identity of salvadorite with kroehnkite. *Notulae Naturae Acad. Nat. Sci. Philadelphia*, no. **72**, 4 pp. (1941).

Salvadorite was described by Herz (*Zeits. Krist.*, **26**, 16–18 (1896)) as a new copper-iron vitriol from Quetena, Chile. Material from the same locality is found by Gordon to agree in crystallography and optical properties with kroehnkite, and to contain 16% $Na_2O$. Salvadorite had, therefore, the physical and crystallographic properties of kroehnkite. Herz's analyses gave $(Cu, Fe)SO_4 \cdot 7H_2O$, like pisanite. Whether the analyses were erroneous, or made upon another mineral (perhaps pseudomorphs) is problematical.

M. F.